GCA TECHNICAL REPORT NO. 66-13-N

ION-MOLECULE REACTION RATES IN AN OXYGEN-NITROGEN ATMOSPHERE

PETER WARNECK

GCA CORPORATION
Bedford, Massachusetts

FINAL REPORT

CONTRACT NO. NAS5-9161

PREPARED FOR
NATIONAL AERONAUTICS AND SPACE ADMINISTRATION
GODDARD SPACE FLIGHT CENTER
GREENBELT, MARYLAND

JULY 1966

GCA Technical Report No. 66-13-N

ION-MOLECULE REACTION RATES IN AN OXYGEN-NITROGEN ATMOSPHERE

Peter Warneck

FINAL REPORT

Contract No. NAS5-9161

July 1966

GCA CORPORATION
GCA TECHNOLOGY DIVISION
Bedford, Massachusetts

Prepared for

NATIONAL AERONAUTICS AND SPACE ADMINISTRATION
Goddard Space Flight Center
Greenbelt, Maryland

TABLE OF CONTENTS

LIST OF ILLUSTRATIONS

LIST OF ILLUSTRATIONS (Continued)

ION-MOLECULE REACTION RATES IN AN OXYGEN-NITROGEN ATMOSPHERE

by
Peter Warneck
GCA Corporation, GCA Technology Division
Bedford, Massachusetts

SUMMARY

The use of a photoionization mass spectrometer for ion-molecule reaction studies is described. Ion source pressures up to 200 microns are employed, measured directly with a McLeod gauge. A method is described for determining ion residence time in the ion source at constant repeller field, using a pulsed light source. Drift velocities, diffusion coefficients, and ion temperatures are given vor N_2^+ ions in air as derived from an analysis of ion pulse shapes. Rate constants or their upper limits are determined for fourteen reactions of atmospheric significance. These include reactions of lithium, argon, nitrogen, oxygen, and hydrogen ions with various atmospheric constituents.

INTRODUCTION

This is the final report under Contract No. NAS5-9161. The principal aim of this program was the measurement in the laboratory of rate constants associated with the ion-molecule reactions

$$(1)\quad N_2^+ + O_2 \rightarrow O_2^+ + N_2$$

$$(2)\quad N_2^+ + O_2 \rightarrow NO^+ + NO$$

$$(3)\quad O_2^+ + N_2 \rightarrow NO^+ + NO$$

These reactions are considered of importance in the D region of the Earth's ionosphere. A novel photoionization mass spectrometer technique has been used in the present work to study these reactions. The rate constant for reaction (1) has been determined. The other two reactions were found to be so slow that only upper limit rate constants could be derived.

In addition to reactions (1) through (3), several other reactions have also been investigated. Most were found to be charge transfer reactions and include the reactions of nitrogen ions with carbon dioxide and nitric oxide, and helium ions with nitrogen and oxygen. All reactions investigated under this contract and the associated measured rate coefficients are listed in Table 1.

TABLE 1

ION MOLECULE REACTION RATES

Reaction	Rate Constant (cc/molecule sec)
1. $N_2^+ + O_2 \rightarrow O_2^+ + N_2$	1.1×10^{-10}
2. $N_2^+ + O_2 \rightarrow NO^+ + NO$	$< 3.0 \times 10^{-14}$
3a. $N_2^+ + 2\ N_2 \rightarrow N_4^+ + N_2$	8.5×10^{-29}
4. $O_2^+ + N_2 \rightarrow NO^+ + NO$	$< 3.0 \times 10^{-15}$
5. $H_2^+ + H_2 \rightarrow H_3^+ + H$	1.8×10^{-9}
6. $He^+ + N_2 \rightarrow N_2^+ + He$	7.1×10^{-10}
7. $He^+ + N_2 \rightarrow N^+ + N + He$	7.6×10^{-10}
8. $He^+ + O_2 \rightarrow O_2^+ + He$	$< 2.0 \times 10^{-10}$
9. $He^+ + O_2 \rightarrow O^+ + O + He$	1.2×10^{-9}
10. $A^+ + O_2 \rightarrow O_2^+ + A$	1.1×10^{-10}
11. $A^+ + CO_2 \rightarrow CO_2^+ + A$	7.0×10^{-10}
12. $N_2^+ + CO_2 \rightarrow CO_2^+ + N_2$	9.1×10^{-10}
13. $N_2^+ + NO \rightarrow NO^+ + N_2$	4.8×10^{-10}
14. $O_2^+ + NO \rightarrow NO^+ + O_2$	7.7×10^{-10}

This report is divided into two parts. The first gives a description of the photoionization mass spectrometer technique; the method used to determine parent ion residence times; and the results obtained with air, nitrogen and hydrogen in the 10 to 200 micron pressure region. This investigation includes the work required under the work statement. The second part of this report gives results for several charge transfer reactions which were studied at pressures 0 to 50 microns using a modified technique.

The use of photoionization for ion production rather than the more common electron impact ionization results in several experimental advantages which have been stressed in several monthly reports under this contract. It may be stated that the overriding feature of the photoionization technique is the ease with which ionizing energies can be selected with a monochromator of only moderate resolving power. To indicate the available energy resolution, it may be noted that at 750Å wavelengths a spectral width of 5Å corresponds to 0.1 eV energy spread. This convenient mode of ionizing energy selection permits operations near the threshold of a selected ionization process, so that the degree of fragmentation can easily be controlled. Another advantage is that the hot filament is not needed and ion sources can be at room temperature. When these sources are at room temperature the pyrolysis of delicate substances is eliminated and the generation of impurities by chemical reactions with the hot filament is excluded.

REACTIONS IN AIR, NITROGEN, AND HYDROGEN

Definitions and Experimental Requirements

The significance of ion molecule reactions in fields as diverse as gas discharge phenomena, mass spectrometry, radiation chemistry, upper atmosphere physics, and flame ionization has stimulated a surge of investigations concerned with ion reaction kinetics, as evidenced by several recent reviews [1-5].* Much of this work has been concerned with the interpretation of reaction mechanisms and the associated or energetics. Relatively few rate constants have been determined.

Aside from interest in the fundamental behavior of ions in high pressure ion sources, the emphasis in the present work is predominantly on the determination of phenomenological rate constants. The corresponding basic experimental requirements may be briefly reviewed. The rate constant k associated with the reaction

$$N^+ + A \rightarrow M^+ + B$$

is defined by the rate equation

$$-\frac{dN^+}{dt} = \frac{dM^+}{dt} = k\, N^+ A \qquad (1)$$

or by the equivalent integrated expression valid for the case when the neutral reactant concentration remains essentially constant

$$k = \frac{1}{A\tau} \log \frac{N_o^+}{N^+} = \frac{1}{A\tau} \log \frac{N_o^+}{(N_o^+ + M_o^+ - M^+)} \qquad (2)$$

Here, the symbols N^+, M^+, and A stand for the concentrations of the respective species, N_o^+ is the initial concentration of the parent ion, and τ is the average residence time of the parent ion N^+ in the source. Clearly, the experimental parameters to be measured for a determination of k include the partial pressure of A, the ratio of ion currents N_o^+/N^+ or N_o^+/M^+, and the residence time τ. Of these, the measurement of τ is most problematic and deserves comment.

At sufficiently low pressures in the source, the ions moving in the extraction field are accelerated freely without impeding collisional encounters, so that the residence time can be calculated from Newton's equation of motion,

*All numbers in [ ] represent reference numbers.

provided the electric field strength and the flight distance are known. This has been the basis for most rate constant determinations in the past. Usually, little uncertainty exists concerning the flight distance, but the fields as calculated from the applied potentials can be distorted by contact potentials, surface charges, or field penetration into the source. The experimental determination of actual fields in the source is difficult and apparently has not been attempted. As the pressure in the source is increased, ions suffer collisions on their way to the extraction orifice and the discrepancies between real and calculated residence times become more serious. However, at sufficiently high ion source pressure, the motion of ions in the repeller field is drift, and the residence time, in principle, can be calculated again. Nevertheless, current knowledge about drift velocities in many cases cannot be extrapolated toward the conditions existing in the ion source, so that there is a real need for a method to determine experimentally the parent ion residence times, regardless of the environmental conditions in the source.

In view of the importance of residence time determinations, a considerable effort was devoted to this task. Residence times were obtained from delay time measurements made possible by the use of a pulsed light source. Delay time data also provided information on drift velocities, diffusion coefficients, and ion temperatures for N_2^+ in air. The present method when applied to ions moving in a time independent repeller field is quite different from that developed by Talrose and Frankevich [6] who let the ions react in an essentially field-free region and then sampled them with a pulsed extraction field; and from that by Hand and von Weyssenhoff [7] who employed a time-of-flight mass spectrometer.

Apparatus

The general features of photoionization mass spectrometers are well described in the literature [8-12]. Since, the present apparatus, Figure 1, is fundamentally the same as previous arrangements, except for more efficient mass analyzer, only the main components are discussed here. Reference is made to a more complete description elsewhere [13].

Briefly, the following components are involved: a 1/2-m Seya vacuum uv monochromator operated in conjunction with a Weissler-type repetitively pulsed nitrogen spark light source, a stainless steel ion source located at the monochromator exit, a sodium salicylate-coated photomultiplier detector for relative intensity measurements, a 180-degree magnetic analyzer with wedge-shaped air gap, and a 20-stage electron multiplier ion detector followed by a vibrating reed electrometer and strip chart recorder. Differential pumping is employed to achieve ion source pressures up to 200 microns while simultaneously keeping the analyzer pressure in the 10^{-6} torr range.

A cylindrical ion source (Figure 2) is used with ion extraction occurring in axial direction through a 0.7 mm diameter orifice. An appropriately biased repeller plate provides the necessary extraction field. Photoions are formed along the plane of the light beam perpendicular to the cylinder axis. The center of ion formation is located 3 mm away from the extraction orifice. With

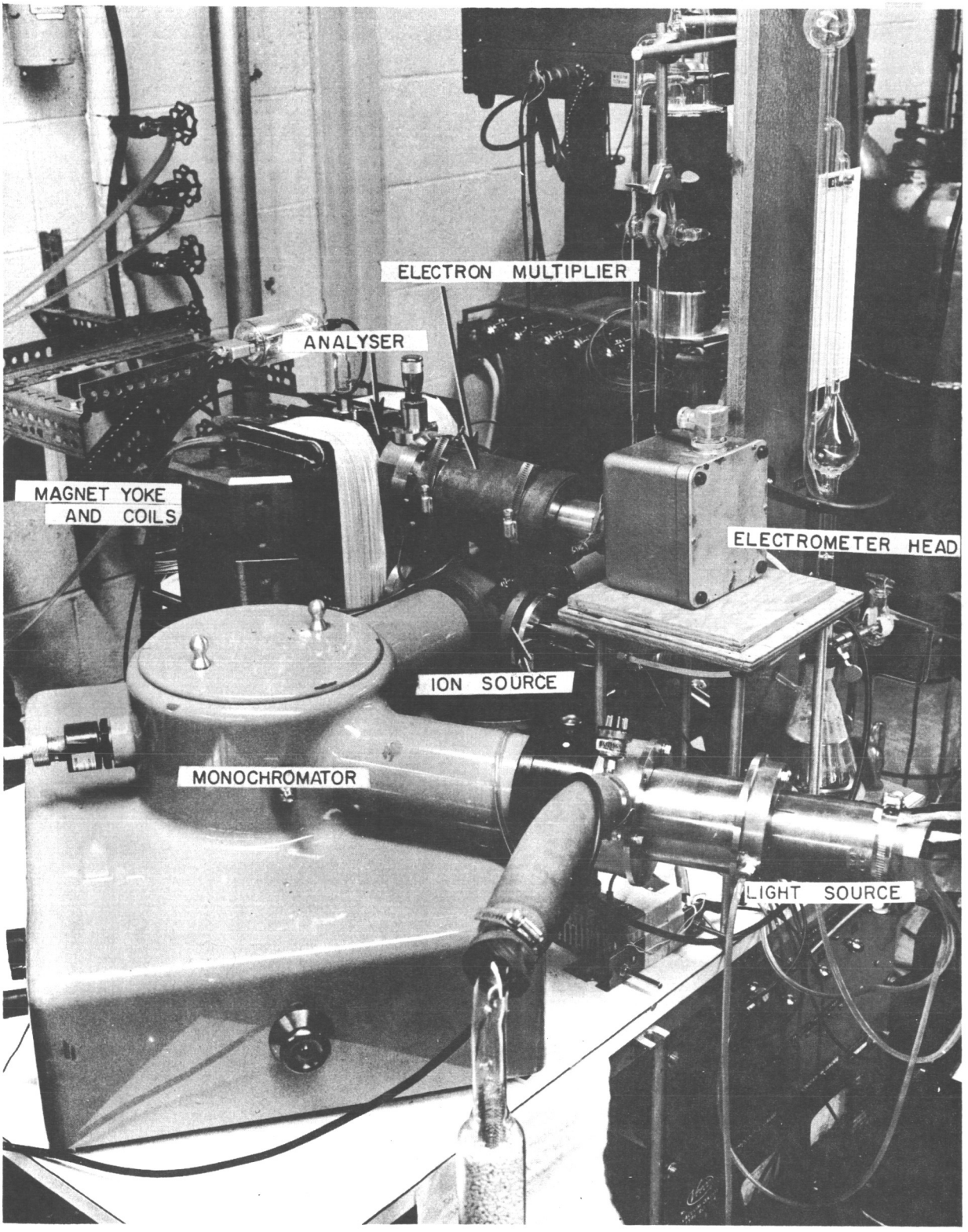

Figure 1. Photoionization mass spectrometer.

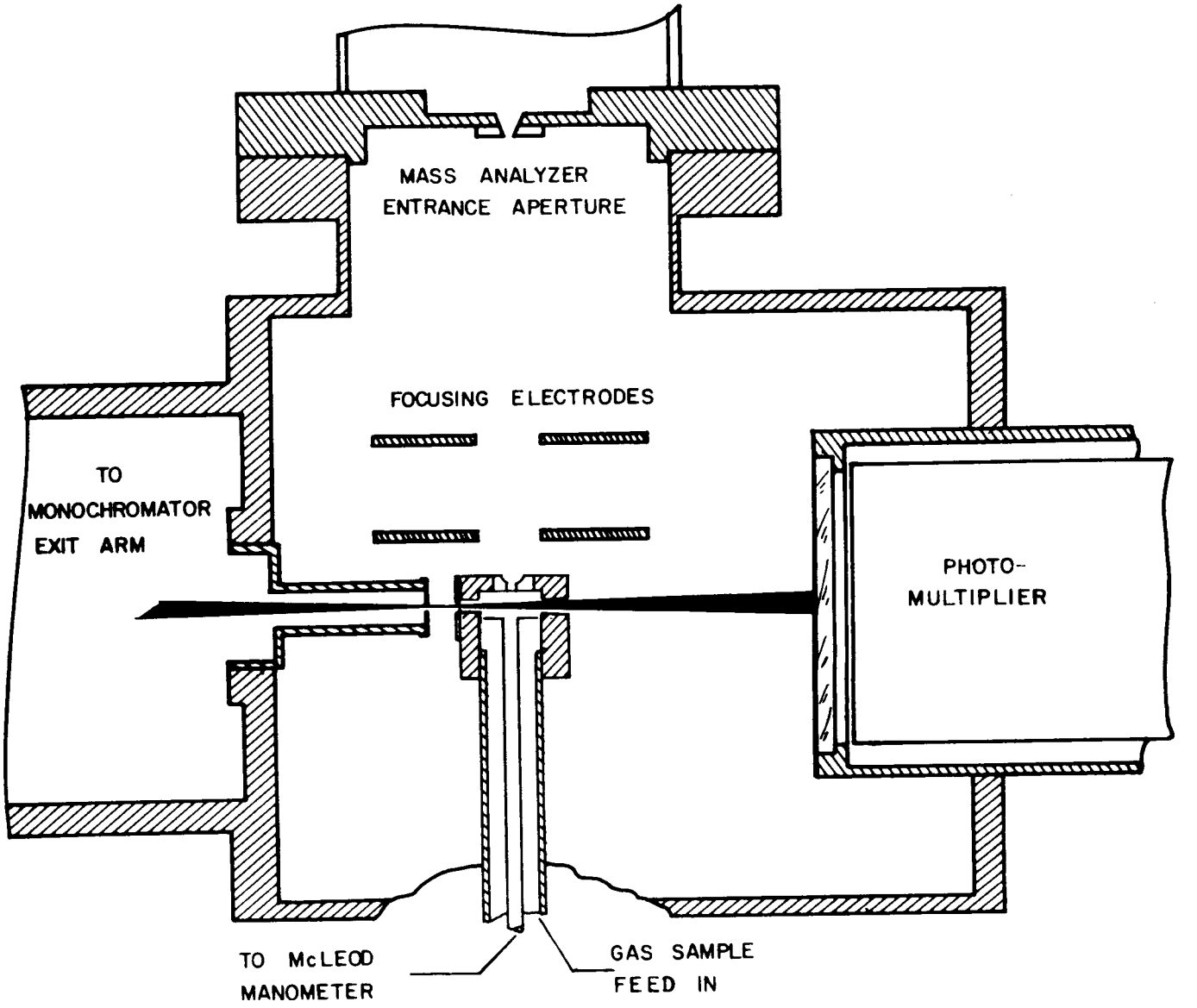

Figure 2. Schematic of ion source.

the optical entrance slit to the source in focal position and with the slit bars adjusted to a width of 0.25 mm, the average width of the light beam inside the source is 0.6 mm. The resulting spectral resolution is approximately 5Å. Subsequent optical slits are wide enough so that the release of photoelectrons from light striking the walls is avoided. Photoelectrons produced at the confining slit are prevented from entering the source by a small auxiliary field.

The gas pressure in the ion source is measured directly with a McLeod gauge through the hollow stem of the repeller. Gases enter the source through the circular gap between the repeller plate and the surrounding walls, and they leave the source mainly through the light beam exit slit. Flow and pressure are adjusted by leak valves. Research quality cylinder gases are employed, with traces of moisture being removed by a trap cooled with liquid nitrogen or dry ice. A cold trap was used also in conjunction with the McLeod gauge.

Determination of Residence Times

The spark light source was operated with a repetition rate of 120 pulses/sec. The average individual pulse duration was less than one microsecond which, in comparison to most ion source residence times, was sufficiently short to justify the notion of essentially instantaneous ion deposition. A notable exception was for hydrogen ions whose residence times were of the same magnitude as the pulse duration.

Ion source residence times were determined from measurements of the total time delay between the formation of ions in the source and their arrival at the mass spectrometer collector. A calibrated Textronix oscilloscope triggered by the phomultiplier signal was used for this purpose. A reproducibility of ± 0.2 microsecond was achieved in these measurements. The total delay time thus obtained is a composite of the residence time of ions in the source and the ion flight time in the mass spectrometer. However, the residence time strongly varies with the repeller field, whereas the ion flight time is nearly independent of the repeller field within certain limits. An extrapolation toward infinite repeller fields, corresponding to negligible residence times, thus provides the ion flight time in the spectrometer which can then be applied to derive the residence time for any chosen repeller potential setting. Figure 3 illustrates this extrapolation. The measured variation of delay time with repeller voltage for a given ion source pressure is plotted versus the inverse repeller voltage. The ion flight time is determined from the intercept of the curve with the ordinate. Figure 4, which gives results for nitrogen ions in air at various pressures, demonstrates that the extrapolation is essentially linear in the vicinity of the ordinate. This linearity has been found to hold for all ions and pressure regions investigated so far. In view of the square root relationship between residence time and repeller potential at low pressures, the possibility of plotting delay time data versus the square root of the inverse repeller voltage was also tested. Linearity of extrapolation was again observed, as expected, but the extrapolations toward the intercept on the ordinate were somewhat longer and, hence, less certain. A comparison of ion flight times derived from both types of plots gave almost identical results.

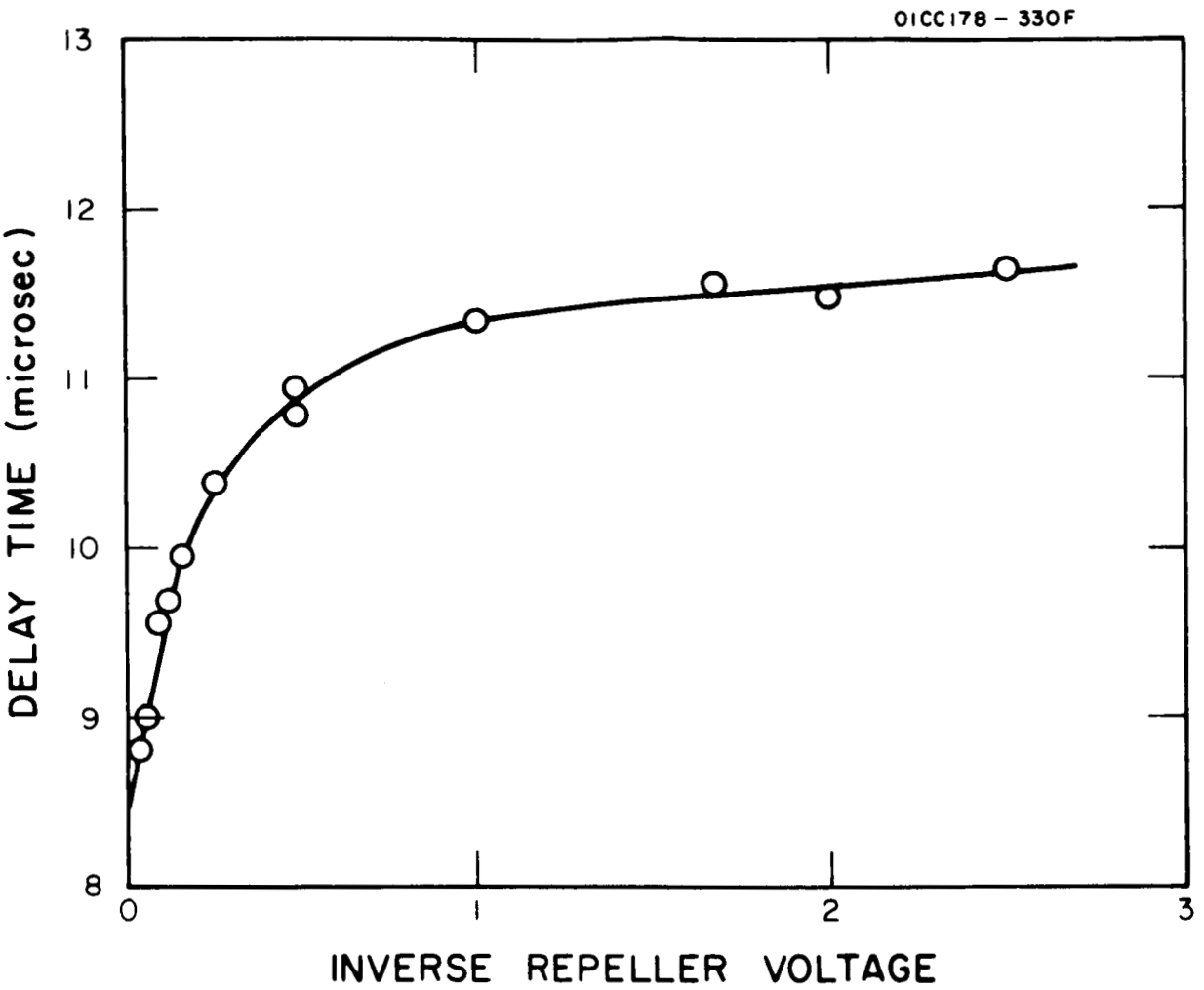

Figure 3. Variation of ion pulse time with repeller voltage. Free flight time is derived from the intercept of curve with ordinate.

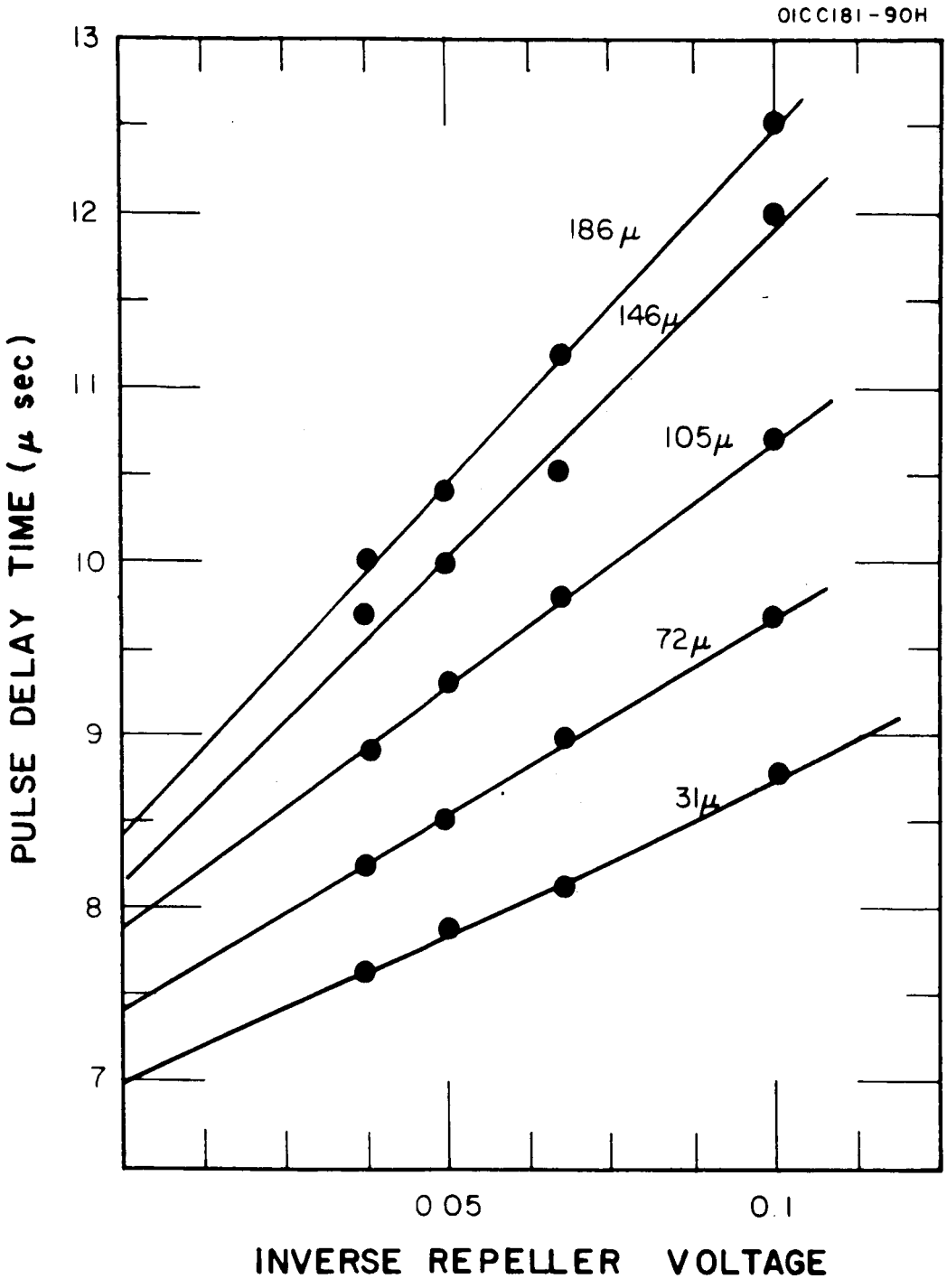

Figure 4. Variation of ion pulse delay times with inverse repeller voltage for various pressures in the source, demonstrating linearity of extrapolation for repeller voltages 10-30 volts.

The ion flight times obtained by these procedures still require a correction, since the assumption that the ion flight time remains unaffected by a change in the repeller potential is valid only for sufficiently small repeller fields. The validity of this assumption breaks down when the ion velocity resulting from acceleration in the repeller field becomes significant in comparison to that required in the accelerating region outside the ion source. The effect to be expected can be calculated from the applied acceleration potential (750 volts) and the approximately known geometry of the ion orbit, resulting in a correction factor 0.94 for ion flight times determined from both types of plots discussed above. It was also established, by these calculation, that the repeller potentials actually applied in the experiments (0-30 volts) were well within the range of repeller potentials for which extrapolations are valid.

For the interpretation of residence time measurements, it is also necessary to discuss the behavior of ion pulse shapes displayed by the oscilloscope. Figure 5 shows the observed and expected pulse shapes for two density distributions perpendicular to the plane of ion formation in the ion source. The rectangular shape on the left corresponds to the initial ion distribution produced by the light beam. The associated idealized pulse shape was observed whenever pressures were sufficiently low and repeller voltages sufficiently high so that residence times were short. For long resindence times, as they were observed at pressures above 50 microns and with low repeller voltage settings, the pulses developed long feet and their shape corresponded better to the Gaussian distribution shown in Figure 5 on the right. At high pressures, when the ions traveling toward the source exit suffer many collisions, the broadening of the initially rectangular ion distribution is interpreted as being due to diffusion. At low pressures when ionic motion is not hampered by collisions, the change in the ion density profile must be produced by the influence of the thermal distribution of initial ion velocities. The influence of charge repulsion is negligible for the ion densities encountered in these experiments.

From Figure 5, it is apparent that the center of the ion distribution is represented by the half-rise point of the charge buildup at the detector. Accordingly, the average residence times should be determined from the half-rise time of the ion pulse observed on the oscilloscope. Unfortunately, the measurement of half-rise times was not always found convenient because of the presence of jitter and statistical noise, particularly for low ion currents. An additional uncertainty is introduced by the finite time constant of the RC element connecting the mass spectrometer collector to the oscilloscope, so that the pulse height against which the half-rise point is to be measured is lowered.

These difficulties are avoided when the pulse onset is used for time delay measurements. However, the use of first arrival times provides only a lower limit to the delay and residence time, and the derivation of average residence times consequently requires a correction to take into account the broadening of the ion distribution. Appropriate correction formulae are derived in Appendix A. In the high pressure domain, where pulse broadening is caused by ion diffusion, the average residence time τ_o can be expressed by

$$\tau_o = \tau/(1 - 1.28\sqrt{2D\tau/d}) \qquad (3)$$

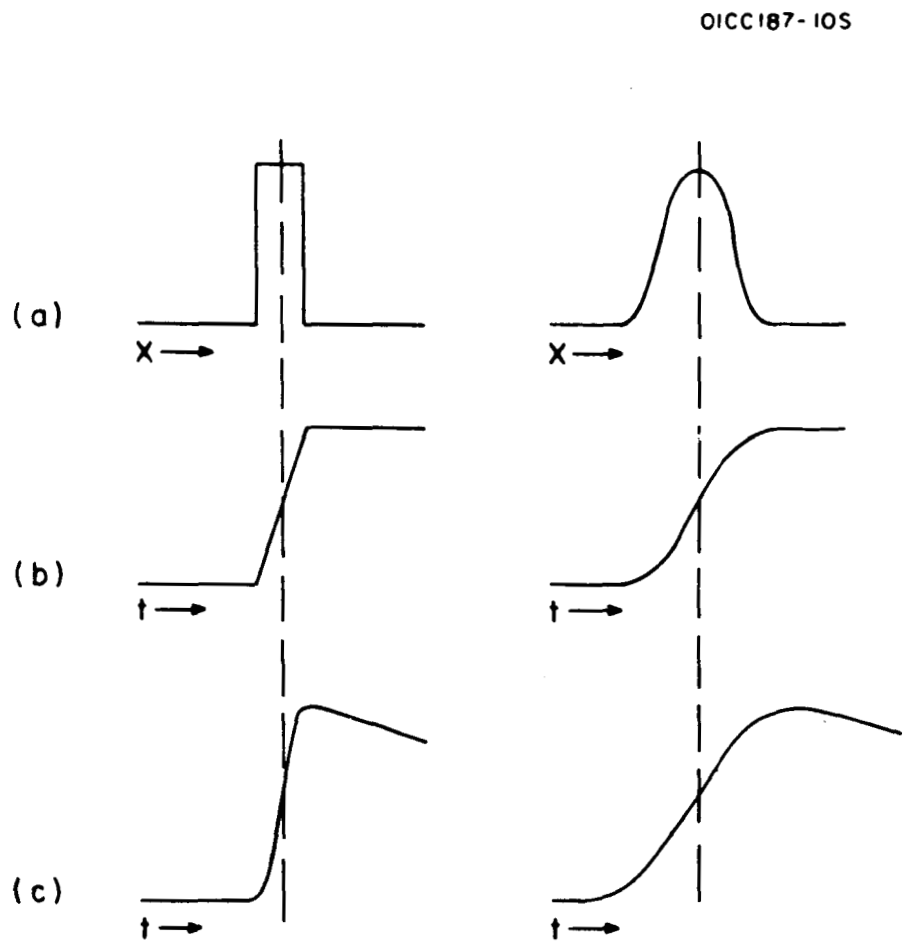

Figure 5. Spatial ion distributions (a) and associated pulse shapes (ideal (b) and observed average (c)). Left for rectangular ion distribution; right for Gaussian distribution.

Here, τ is the lower limit residence time derived from the first arrival of the ion pulse, D is the diffusion coefficient of ions under consideration, and d is the distance from the origin of these ions to the ion source exit. A similar formula is applicable at low pressures where the pulse broadening is due to initial thermal velocities of the ions:

$$\tau_o^2 = \tau^2 / \left(1 - 1.28\, \tau \sqrt{\frac{kT}{m}}\, \frac{}{d}\right) \qquad (4)$$

with k being the Boltzmann constant, T the gas temperature, and m the mass of the ionic species under consideration.

Performance of Apparatus

It is commonly assumed for ion-molecule reactions studies that ion current ratios measured at the mass spectrometer detector are equivalent to the ratios of ion fluxes generated in the source. Several fundamental effects, however, can invalidate the assumption of equal collection efficiencies for all ions. The factors discussed here include pressure, ion-electron conversion at the multiplier detector, and the variation of ion collection from the source for ions with different kinetic energies.

The use of high pressures in a mass spectrometer ion source generally leads to ion current-pressure relationships which are nonlinear, even in the absence of ion-molecule interactions. Such nonlinearities were observed to occur in the present experiments, mainly at pressure exceeding 100 microns. Predominantly, the cause is non-uniform absorption of ionizing radiation in the source. This effect has been discussed previously. [13] If absorption cross sections are available for the wavelength region of interest, appropriate corrections can be applied. It appears, however, that several other effects can also contribute to the observed nonlinearity of ion current with pressure. The following possibilities were explored: (a) dependence on light intensity, (b) variation with repeller potential, and (c) broadening of mass peaks. These studies were made with oxygen in the ion source as no ion-molecule reactions were observed to occur for O_2^+ ions in O_2 up to 200 microns pressure.

Dependence on light intensity. - To study the influence of light intensity but keep the other parameters constant, it was necessary to adjust intensities by variation of the monochromator entrance slit setting. Since this procedure affects the resolution, the 685Å group of nitrogen lines were used for the measurements. This group consists of an unresolved triplet well isolated from other lines in the vicinity. Accordingly, any effects caused by a change of the effective absorption cross section are minimized. At 685Å, the energy is still insufficient to produce dissociative ionization of O_2 so that only O_2^+ ions are present. Photomultiplier currents were used as a measure of the light intensity. The results are shown in Figure 6, where the observed ion currents divided by the photomultiplier currents are plotted as a function of ion source pressure. A lowering of the normalized ion currents is apparent at pressures above 100

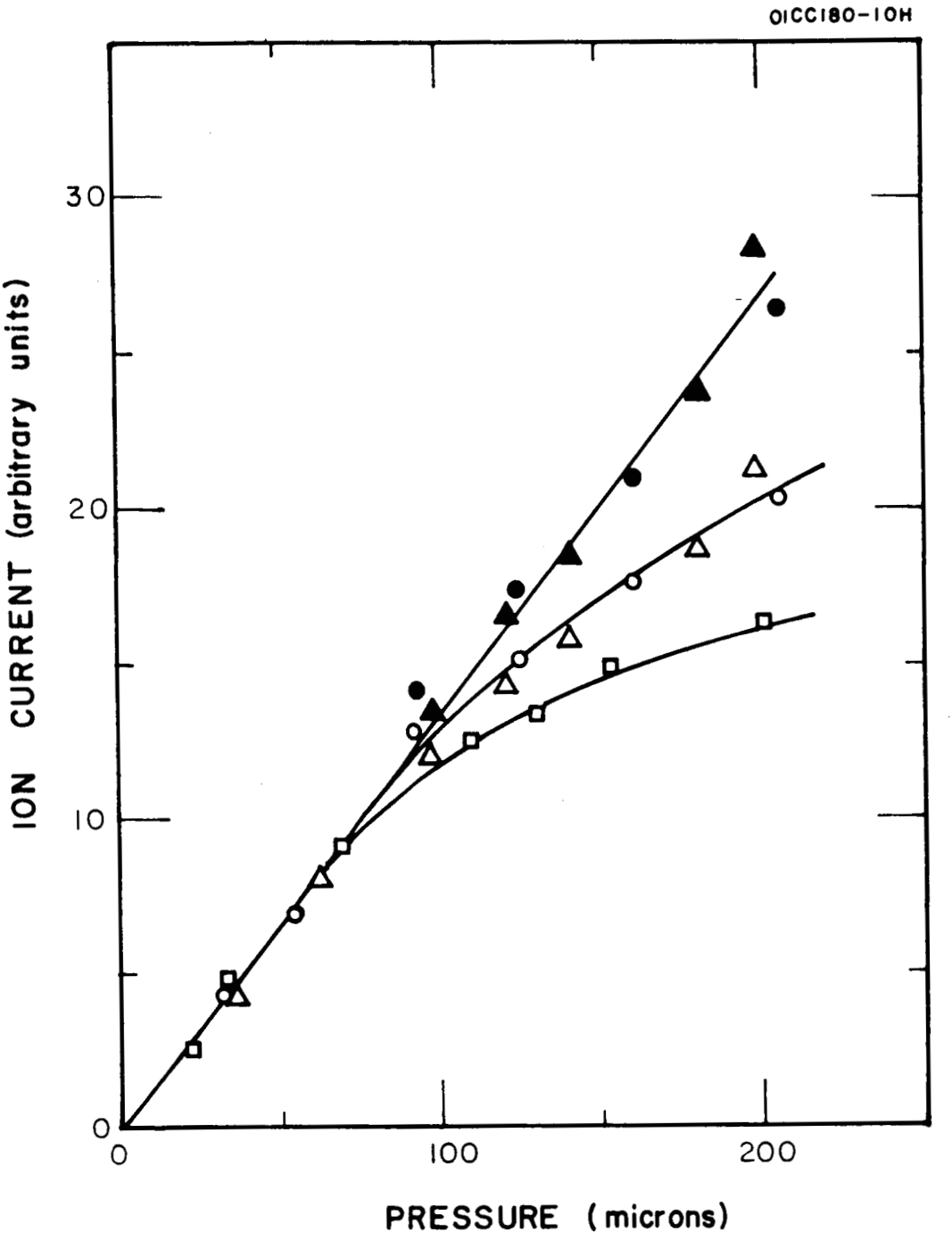

Figure 6. Mass 32 ion currents in oxygen normalized with respect to incident light intensity as measured by photomultiplier current: △ — 16 x 10^{-8} amps; — 111 x 10^{-8} amps; — 325 x 10^{-8} amps. Filled-in symbols signify absorption corrected data.

microns when a high light intensity is used. The reason for the intensity dependence is not entirely clear, but it may be noted that with the use of pulsed light sources as in the present experiments, transient ion densities of the order of 10^8 ions/cc can be reached so that space charge effects might become significant. The study of ion-molecule reactions obviously requires operation at lower light intensities where this effect is negligible.

Variation with repeller potential. - Variation of the repeller potential causes a variation of the ion intensity at any ion source pressure owing to a change in the ion collection efficiency. When adjusting for this effect, it was found that a variation of the repeller potential had no influence upon the ion intensity as a function of pressure for the investigated range of repeller potentials, 1 to 10 volts, corresponding to field strength of approximately 1.6 to 16 volts/cm.

Broadening of mass peaks. - Since ion currents customarily are measured at the maximum rather than by the area underneath a mass peak, it was of interest to investigate the equivalence of both procedures. This test was again performed with ionizing light at 685Å. The data shown in Figure 7 are normalized with respect to each other to facilitate comparison. Up to 120 microns, the data are equivalent but at higher pressures, the use of peak heights gives lower relative values. At these pressures, the mass peaks develop tails in the direction of lower energies. These tails indicate an increase in the energy spread of the ions which undoubtedly is caused by energy losses during ion-neutral collisions in the accelerating region outside the ion source. Other effects produced by collisions include a broadening of the ion beam and loss of beam intensity due to self scattering. The last two processes, however, have little influence upon the ion current in the present experimental arrangement because of the large solid angle of acceptance associated with the employed magnetic analyzer.

For the study of ion-molecule reactions, it is also imporant to establish the signal conversion efficiency of the electron multiplier detector for ions of different mass (and type), since ion discrimination would affect the observable reactant-product ratios. Owing to the small ion currents available in the present experiment, this effect could not be evaluated directly. However, at sufficiently low source pressures, ion production is proportional to the product $\gamma\sigma p$, where γ is the photoionization yield, σ the absorption cross section at the employed wavelength, and p is the gas pressure in the source. Hence, it should be possible to estimate the relative multiplier conversion efficiencies from a comparison of ion currents observed for various gases and corrected for the pertinent values of $\gamma\sigma p$, provided the ion collection from the source is independent of the nature of the ions. Appropriate experiments with 685Å radiation employed argon, nitrogen, oxygen, carbon monoxide, carbon dioxide, hydrogen, and methane as sample gases. Photoionization yields and absorption cross sections for the first five gases were taken from the tables given by Samson and Cairns, [14] those for hydrogen and methane from the data by Cook and Metzger. [15,16] Although the results for relative multiplier conversion efficiencies showed considerable scatter due to the accumulation of various errors, they displayed no trends within the investigated m/e region indicating that mass discrimination, if present, is a small effect. This is consistent

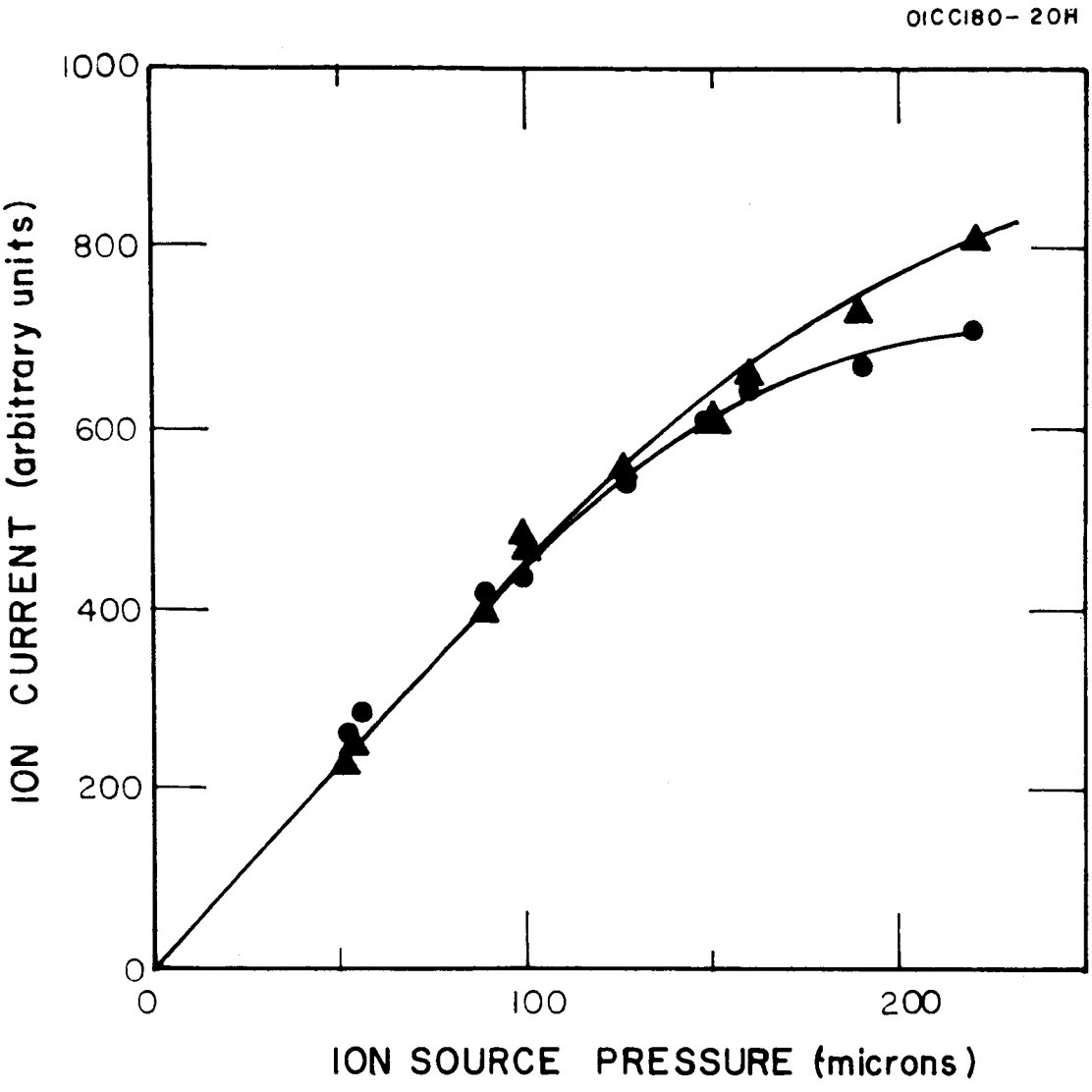

Figure 7. Mass 32 peak height (●) and peak area (▲) for oxygen as a function of pressure. Data normalized with respect to each other.

also with previous data obtained with 584Å helium resonance radiation [13]. It is noteworthy that, in both cases, the response of the detector for methane ions was persistently higher relative to that for the other sample gases, if the fragmentation yield for CH_3 and CH_2 ions [17] was taken into account.

While these results appear to justify the assumption of equal collection efficiencies for all ions present in the source, there is evidence that the collection efficiency decreases for ions which have acquired excess kinetic energy during a reaction. The balance between reactant consumption and product evolution was standard for the dissociation charge transfer process involving helium ions and nitrogen or oxygen. These reactions were discussed by Ferguson et al. [18] and by Moran and Friedman [19]. The details of this experiment will be reported below in the section that deals with charge transfer reactions. It is significant that the reaction of helium ions with nitrogen gave product ion intensities in perfect balance with helium ion losses, whereas in the reaction with oxygen when studied at low pressures, only 20 percent of the consumed helium ions could be recovered as O^+ ions. No other products were discernible. As the gas pressure was increased so that O^+ product ions underwent collisions on their path to the extraction orifice, the product-reactant loss ratio was improved. Moran and Friedman [19] have shown that the reaction of helium ions with oxygen results in oxygen ions having excess kinetic energies. This finding has been confirmed in the present work by means of retarding potential measurements. On the other hand, the reaction with nitrogen is essentially thermoneutral so that the resulting products are in the thermal kinetic energy range. The present results, therefore, lead to the conclusion that the employed ion source geometry and low electric fields disfavor the collection of ions endowed with excess kinetic energies. The influence of this factor is greatest at low pressures, but it is subdued when ion neutral collisions are sufficient to moderate the energy excess.

Residence Times for N_2^+ in Air

Figure 8 gives the variation of residence times with pressure for nitrogen ions in air with a repeller potential of 1 volt. Of the two sets of data shown, the upper one was obtained from the half-rise time of the ion pulse and represents the true average residence times, whereas the lower refers to the earliest arrival times of the ion pulse. The observed decrease of residence times with decreasing pressure is expected. Extrapolation toward low pressures gives a limiting value which is in reasonable agreement with the residence time calculated from the equation for collision-free acceleration of the ions (3.3μ sec). From the data shown in Figure 8, drift velocities of nitrogen ions in air, their diffusion coefficients, and the associated ionic temperatures can be deduced.

Drift velocities were obtained from the relation $v = d/\tau_o$ and are shown in Figure 9 in a logarithmical plot versus the relative field strength E/p. The observed slope of nearly 1/2 indicates a root relationship. Also shown by the solid and broken lines are results reported by Martin et al. [20] and by

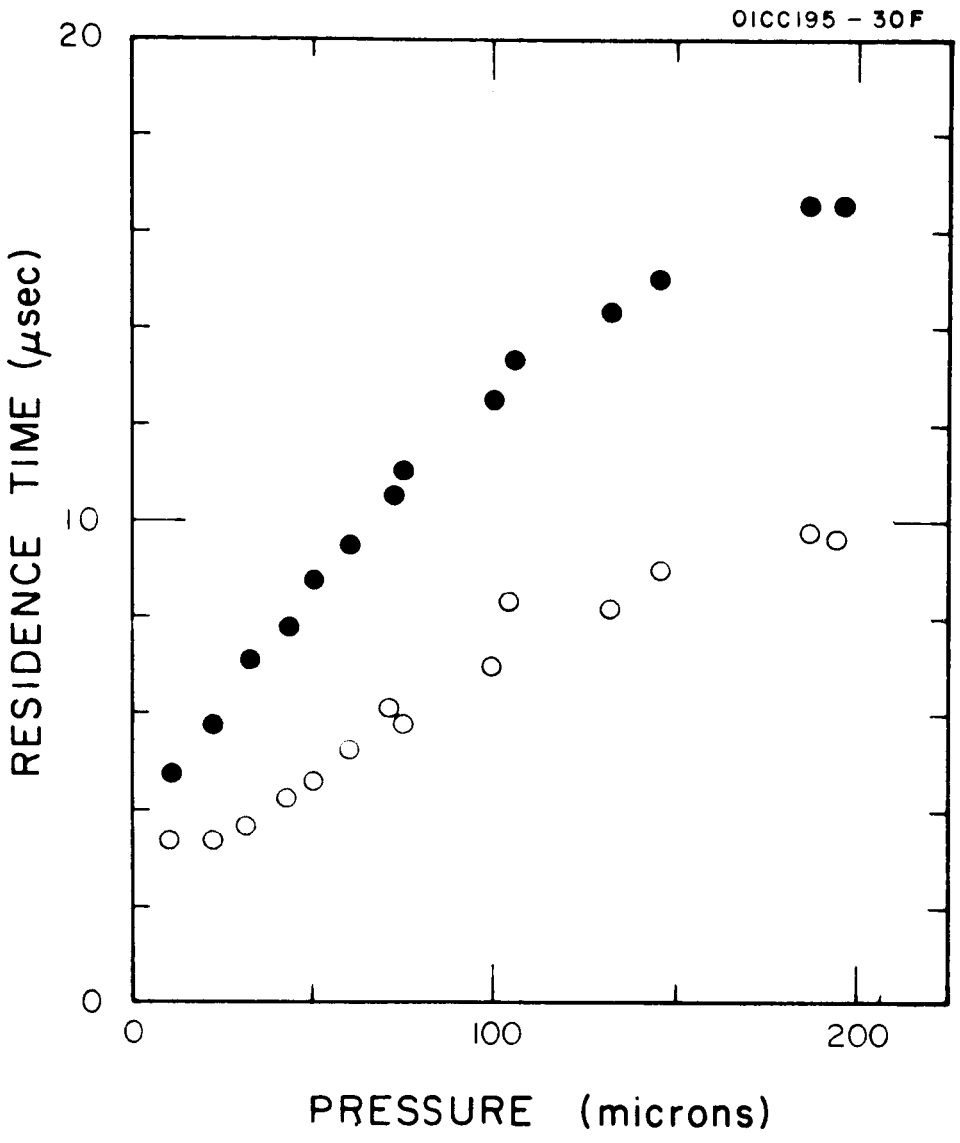

Figure 8. N_2^+ ion residence times in air as a function of pressure, derived from first arrival time (○) and half rise time (●) of ion pulse at the collector.

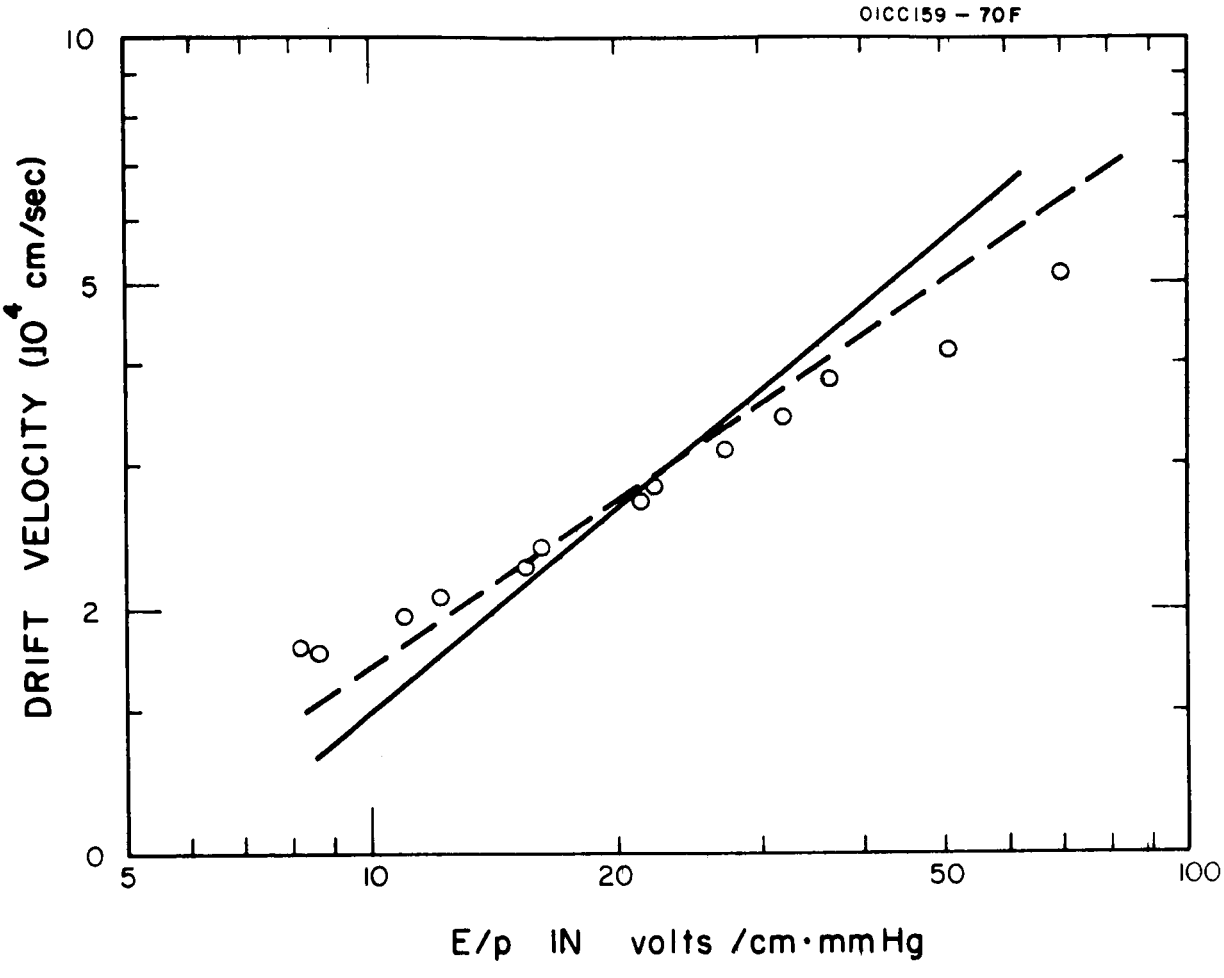

Figure 9. Drift velocities of N_2^+ ion in air as deduced from residence times in the source. Circles indicate present data; the solid line data by Martin, et al., the broken line data by Dahlquist.

Dahlquist [21] for N_2^+ ions in nitrogen. Good agreement is obtained even though the present results refer to air. Nevertheless, our data are considered only moderately accurate because of the difficulties involved in defining the true electric field. At E/p values greater than 45, the data are even less acceptable since the pressures become too low to justify the model of drift.

Diffusion coefficients were calculated from τ and τ_o with the aid of Equation (3). The results are shown in Figure 10 as a function of reciprocal pressure. The observed linear relationship confirms the interpretation that the broadening of the ion density profile in the ion source is due to diffusion. The here derived diffusion coefficients have the expected gas kinetic values. The linear relationship with 1/p breaks down for pressures less than 40 microns, which is also the limit to which meaningful drift velocities could be determined. At lower pressures, the number of collisions an ion encounters on its way to the sampling orifice evidently is insufficient to sustain the mechanisms of diffusion and drift. In this pressure region, the motion of ions changes from drift to free acceleration.

The independent determination of diffusion coefficients in these experiments permits also the derivation of ion temperatures from the relationship $T_i = eD/k\mu$. Here, e is the charge of the ion, k the Boltzmann constant, and $\mu = v/E$ the ionic mobility. Temperatures derived in this way are plotted versus E/p in Figure 11. The large scatter of data is due mainly to the variation in the diffusion coefficients. The solid line shown was obtained with the use of least square averaged diffusion coefficients. It is interesting to note the approximate linearity with E/p. The relationship $T_i = T_{gas} + a\ E/p$ for nitrogen ions in nitrogen was originally proposed by Varney. [22] The slope in Figure 11 is a = 11, which is in excellent agreement with that deduced by Varney (a = 12.5) from drift velocity measurements at different temperatures. However, since Varney derived the temperature scale from considerations of the equilibrium between N_4^+ and N_2^+ ions, his data really refer to the temperature of the N_4^+ ion, although he assumes them applicable also to N_2^+ ions. As a consequence, the obtained agreement may be coincidental. At present, it is not known whether the observed (approximate) linearity of T_i with E/p has general applicability, but from the derivation of the ion temperature it is clear that it should depend on the detailed behavior of ion mobility.

Reaction Rates

In this section, rate constants are reported for the reactions of nitrogen ions with oxygen and nitrogen, and for the proton transfer reaction in hydrogen. More specifically, there reactions read

$$(1) \quad N_2^+ + O_2 \rightarrow O_2^+ + N_2$$

$$(2) \quad N_2^+ + O_2 \rightarrow NO^+ + NO$$

$$(3) \quad N_2^+ + N_2 \rightarrow N_4^+$$

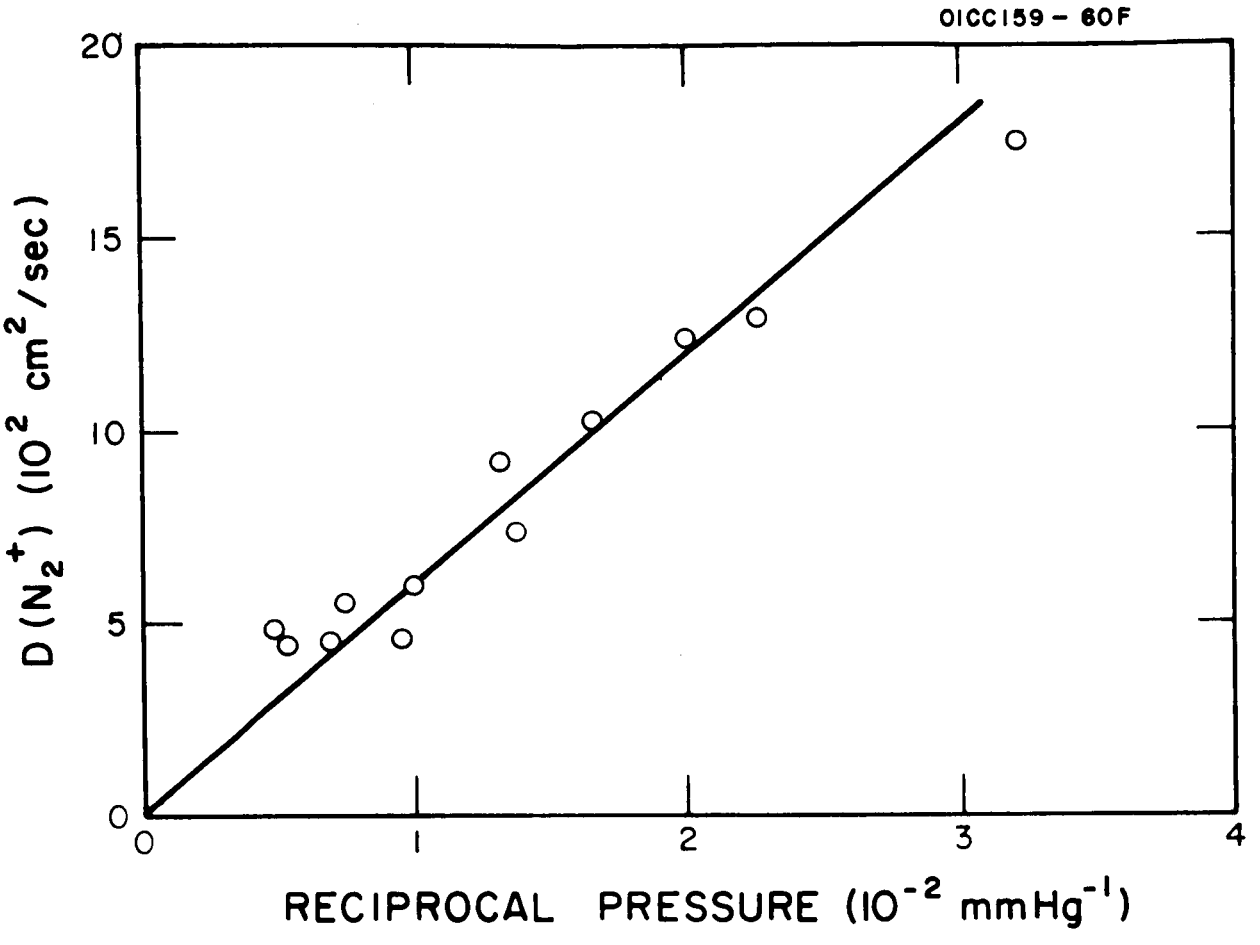

Figure 10. Diffusion coefficients for N_i ions in air as derived from the broadening of the ion profile in the source.

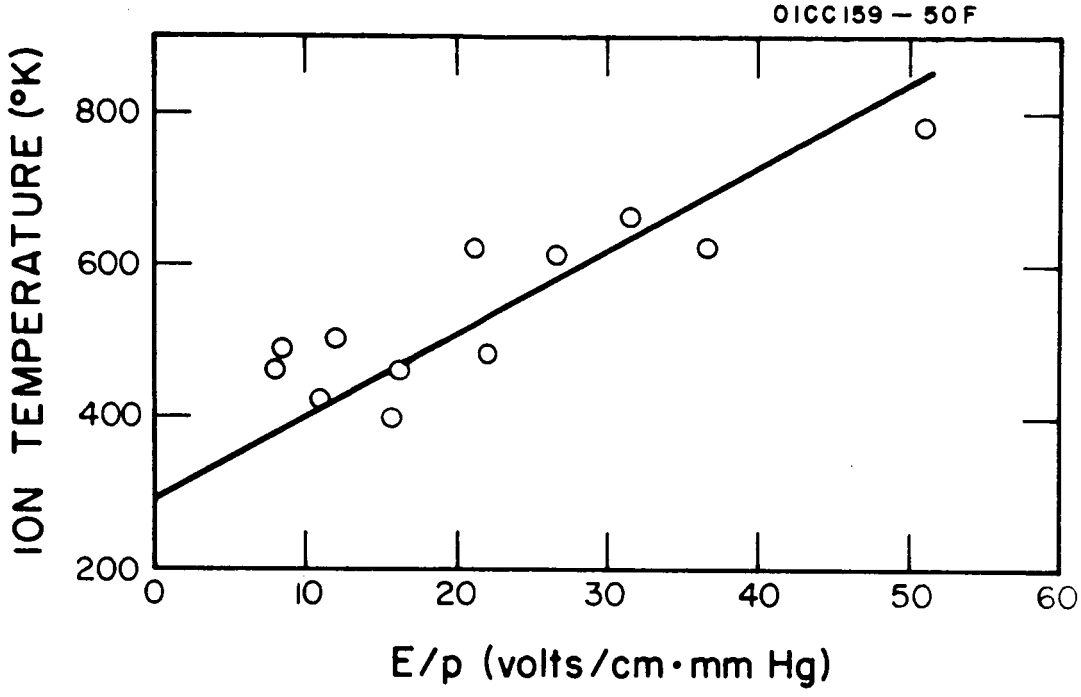

Figure 11. N_2^+ ion temperature in air versus relative field strength E/p.

$$(4) \qquad O_2^+ + N_2 \rightarrow NO^+ + NO$$

$$(5) \qquad H_2^+ + H_2 \rightarrow H_3^+ + H$$

There reactions were studied with radiation centered at 764Å wavelength. Owing to the limited wavelength resolution, the employed radiation contained several component lines, the three strongest being NIV 765.1, NIII 764.4, and OV 760.4Å. The associated energy spread is 0.1 eV. The available photon energy lies 0.64 eV above the threshold for N_2^+ formation and 0.75 eV above that for H_2^+ formation. Although this is insufficient for the production of ions in electronically excited states, the possibility of vibrational or rotational excitation of the ground state cannot be excluded.

Reactions (1) and (2) were studied with air introduced at source pressures up to 200 microns. Reaction (1) proceeded rapidly, while Reaction (2) was negligible under all conditions. Figure 12 shows the N_2^+ and O_2^+ ion currents observed as a function of pressure for a repeller voltage setting of 0.5 volt. Occurrence of Reaction (1) is evidenced by the rise of O_2^+ current at the expense of the N_2^+ current. Also shown in Figure 12 is the sum of both currents which, in this case, exhibits an almost linear pressure dependence. The deviations from linearity are attributable to the increase of light absorption in the source. The limiting ratio of the ion currents at low pressures, $R = i(N_2^+)/i(O_2^+)$, was determined by expansion of Figure 12 as R = 7.1. The ratio expected from the known absorption and photoionization coefficients, [14] taking into account only the three strongest lines contributing to the radiation, weighted according to their intensity, is R = 8.5. The agreement is reasonable if it is considered that the wavelength setting may have favored either one of the outer lines of this group.

Rate constants determined from the data shown in Figure 12 are given in Table 2. The initial ion currents, $i(N_2^+)_o$ and $i(O_2^+)_o$, were deduced from the sum of the observed ion current multiplied by the ratio R measured at low pressures. N_2^+ residence times were determined from first arrival times of the ion pulse at the detector, and the correction according to Equation (3) was applied. The residence times thus found were somewhat smaller than those shown in Figure 8 despite the smaller repeller potential employed. However, these measurements were made early in this work, when a larger extraction orifice was used so that field penetration probably raised the field strength actually existing in the source. The data shown in Table 3 were obtained under conditions more nearly resembling those pertaining to Figure 8. The diameter of the extraction hole in this second series of runs was 0.7 mm (as used throughout in later experiments), and the repeller potential was approximately 1.5 volts. The rate constants obtained from both series of sums are in excellent agreement with each other indicating that the employed method of residence time determination yields correct results independently of repeller potential settings and the resulting fields. Significantly, the individual rate constants exhibit no trends as the pressure is varied, although in Figure 11 the ionic temperature decreases as the pressure in increased. This shows that at least in the 300-700°K region, the rate constant for Reaction (1) is temperature independent.

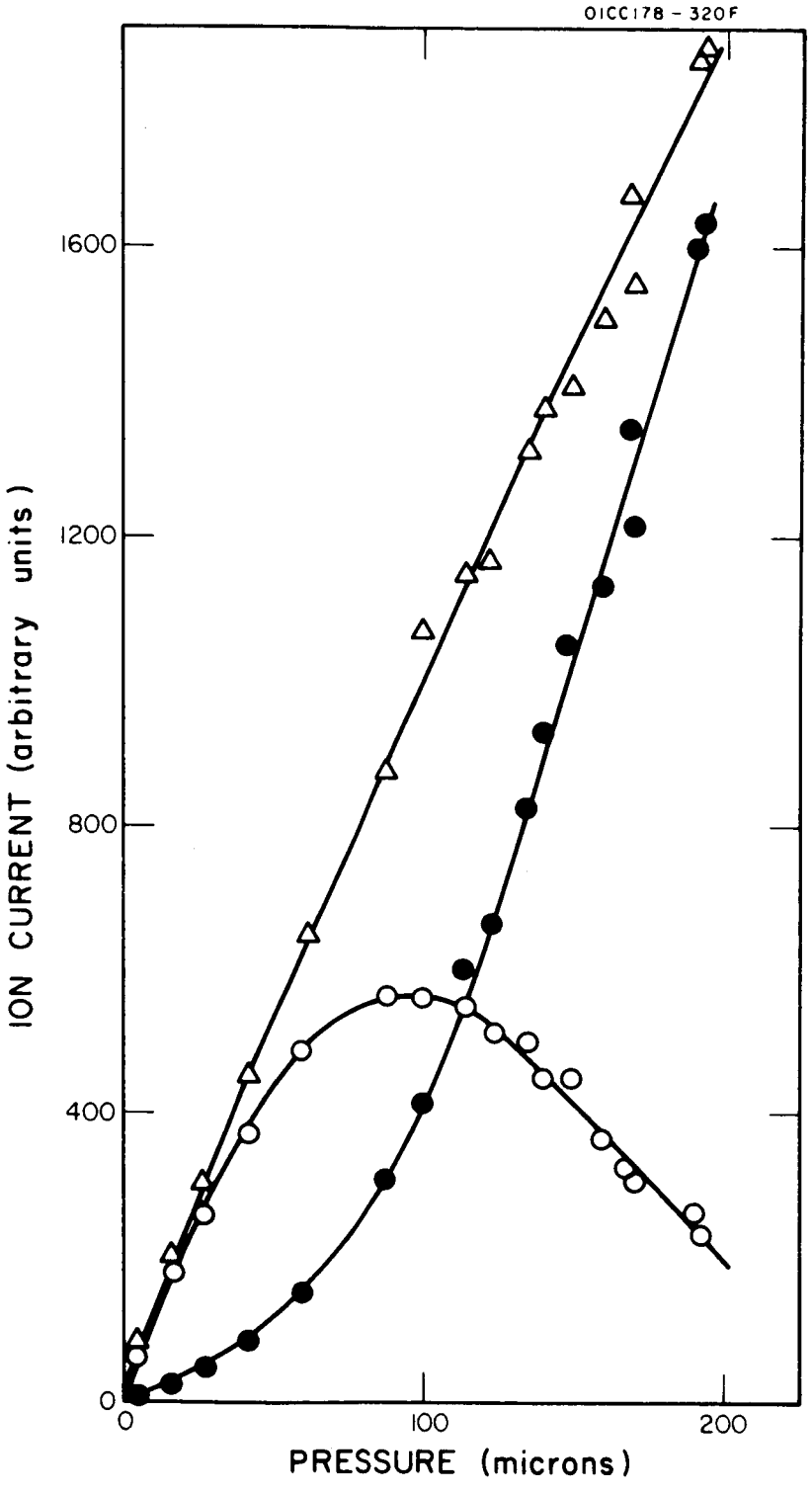

Figure 12. Mass 28 (O) and mass 32 (●) ion currents as a function of ion source Pressure Lines of ion currents indicated by triangles.

TABLE 2

RATE CONSTANTS FOR THE REACTION $N_2^+ + O_2$

P microns	(N_2^+)	(O_2^+)	$(N_2^+)_o$	$(O_2^+)_o$	τ	$\log \frac{(N_2^+)_o}{(N_2^+)_o - \Delta(O_2^+)}$	$k \times 10^{10}$
	(arbitrary units)				μsec		cc/mol sec
41	370	81	396	55	2.6	0.031	1.01
60	490	156	566	80	3.8	0.063	0.96
87	565	310	766	108	5.6	0.134	0.96
100	560	415	854	120	6.8	0.184	0.94
114	550	600	1007	142	7.6	0.263	1.06
123	508	662	1025	144	8.4	0.305	1.22
135	498	830	1162	163	9.6	0.370	0.99
140	450	930	1208	170	10.0	0.431	1.07
149	452	956	1232	173	10.4	0.439	0.99
160	367	1135	1315	185	11.2	0.554	1.07
168	320	1355	1465	207	11.6	0.665	1.19
170	302	1215	1355	191	11.8	0.612	1.06
190	260	1600	1629	239	12.8	0.783	1.12
192	236	1638	1640	231	12.9	0.868	1.22

average $k_1 = 1.06 \times 10^{-10}$ cc/mol sec

TABLE 3

RATE CONSTANTS FOR THE REACTION $N^+ + O_2$

P microns	(N_2^+)	(O_2^+)	$(N_2^+)_o$	$(O_2^+)_o$	τ	$\log \frac{(N_2^+)_o}{(N_2^+)_o - \Delta(O_2^+)}$	$k \times 10^{10}$
	(arbitrary units)				μsec		cc/mol sec
30	480	100	500	70	3.1	0.028	1.07
44	535	144	582	84	3.7	0.048	1.04
66	580	260	735	104	5.3	0.104	1.03
85	530	380	796	112	6.2	0.178	1.18
102	530	485	888	125	7.1	0.226	1.09
128	435	700	994	140	8.4	0.360	1.16
136	410	720	989	139	8.7	0.385	1.14
140	410	765	1030	145	9.0	0.400	1.15
160	335	990	1180	166	9.8	0.521	1.16
176	290	1130	1345	190	10.5	0.521	0.99
196	240	1360	1400	197	11.3	0.771	1.22
200	250	1340	1390	196	11.4	0.752	1.15

average $k_1 = 1.11 \times 10^{-10}$ cc/mol sec

The value averaged from the data shown in Tables 2 and 3 is $k_1 = 1.1 \times 10^{-10}$ cc/mol sec, in approximate agreement with the previous estimate of 2×10^{-10} cc/mol sec by Fite et al., [23] and in excellent agreement with the value $k_1 = 1.0 \times 10^{-10}$ recently established by Ferguson and collaborators [24]. Their experimental results were obtained under entirely different experimental conditions, that is, with a steady state flow technique involving several torr of helium as a buffer gas. The close agreement of results thus adds confidence in the present experimental technique.

Reaction (2) has not been observed in these experiments and only an upper limit to its rate constant can be given. Even at pressures exceeding 200 microns, no nitric oxide ions could be detected. However, in this pressure region, the O_2 peak generated by Reaction (1) developed a tail, a portion of which covered the m/e = 30 region of the mass spectrum. From the current ratio of the background to that of the mass number 32 peak, the upper limit rate constant for Reaction (2) was found to be 3×10^{-4} that of Reaction (1) or $k_2 \leq 3 \times 10^{-14}$ cc/mol sec. This is an order of magnitude smaller than the upper limit value derived by Galli et al., [25]. In this particular case, the photoionization mass spectrometer is used with advantage, since as Talrose [26] has demonstrated, the commonly employed electron impact ion sources generate NO from nitrogen oxidation at the hot filament.

Reaction (3) was studied in nitrogen at source pressures from 90 to 200 microns. At lower pressures, N_4^+ ions could still be discerned, but usable data were difficult to obtain because of excessive noise. Water vapor was a noticeable impurity despite the application of a liquid nitrogen cooled trap. Apparently, the formation of H_2O^+ ions occurs by a very fast charge transfer reaction involving nitrogen ions. The intensity of the m/e = 18 peak was, therefore, used to correct the initial N_2^+ currents required for the determination of rate constants, although the correction amounted to only a few percent. Table 4 shows the data including residence times and rate constants computed from Equation (3). The magnitude of the derived rate constants is in reasonable agreement with that reported by Fite et al., [23] ($k_3 = 5 \times 10^{-13}$ cc/mol sec), but the present data are in disagreement in that they exhibit a trend with pressure. Seemingly, Reaction (3) is not a bimolecular process as predicted by Fite et al. A plot versus pressure in Figure 13 shows that the pressure dependence of the rate constants derived for the bimolecular process is linear and that an extrapolation toward zero pressure goes through the origin of the plot. This is clear evidence that Reaction (3) involves a third body and should properly be written

$$N_2^+ + 2N_2 \rightarrow N_4^+ + N_2$$

In view of the attachment nature of this reaction, the participation of a third body is required to stabilize the resultant N_4^+ ion. However, at sufficiently high pressures, the reaction can become effectively bimolecular if the lifetime of the N_4^+ complex is longer than the mean free flight time of the ions between collisions so that stabilization is always effective. In the pressure range used here, this case evidently does not apply. The rate constants associated with

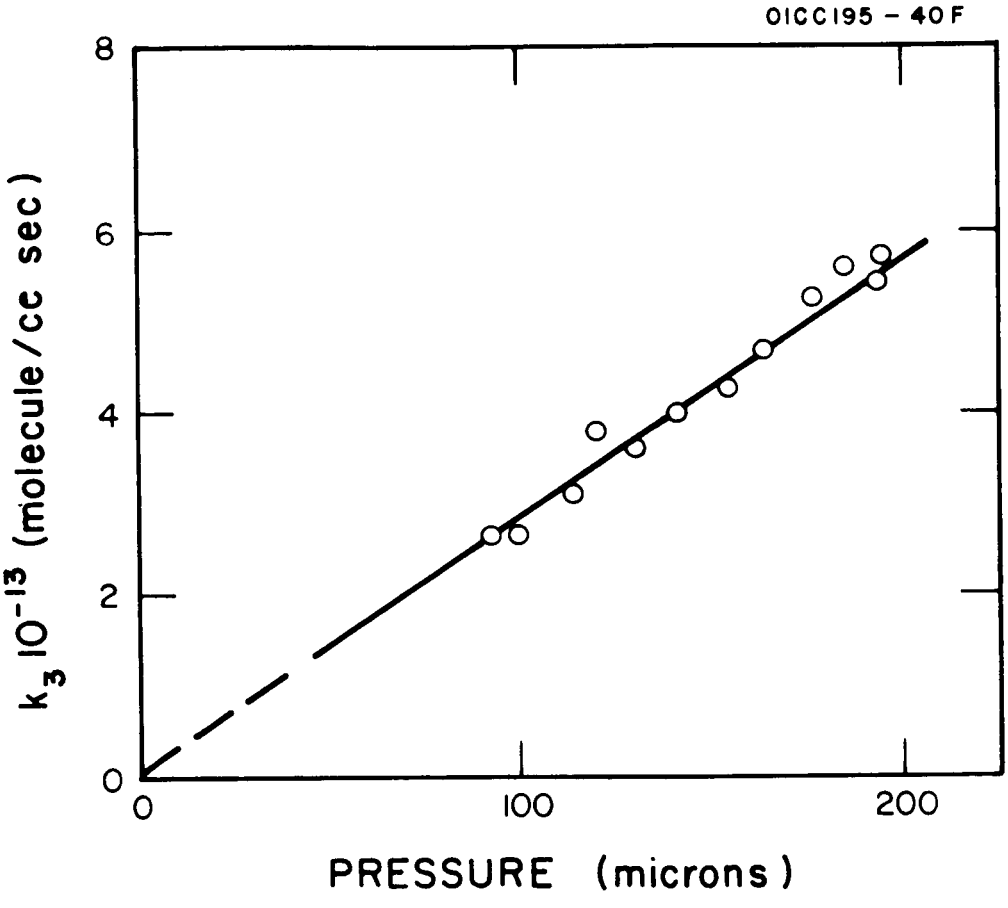

Figure 13. Variation of the rate constant k_3 with pressure.

TABLE 4

RATE CONSTANT FOR THE REACTION $N_2^+ + N_2$

P microns	(N_2^+)	(N_4^+)	N_o	$(N_4^+)/N_o$	τ	$k_3 \times 10^{13}$	$k_{3a} \times 10^{29}$
	(arbitrary units)				μsec	cc/mol sec	cc^2/mol^2 sec
94	1330	11	1365	0.0082	10.0	2.61	8.42
98	1290	12	1302	0.0092	10.5	2.71	8.38
115	1420	20	1440	0.0139	11.8	3.10	8.18
120	1400	27	1460	0.0185	12.2	3.84	9.30
130	1470	30	1500	0.0200	13.0	3.60	8.40
142	1510	40	1550	0.0258	13.8	4.00	8.55
154	1560	51	1611	0.0317	14.6	4.27	8.40
165	1510	64	1616	0.0406	15.4	4.73	8.70
177	1560	81	1691	0.0492	16.0	5.27	9.02
185	1540	96	1686	0.0588	16.6	5.62	9.20
194	1510	108	1666	0.0668	18.7	5.45	8.50
195	1515	111	1686	0.00617	17.2	5.75	8.85

N_o = sum of ion intensity at m/e = 28, 56, and 18

average $k_{3a} = 8.5 \times 10^{-29}$ cc^2/mol^2 sec

Reaction (3a) are obtained from the bimolecular rate constants k_3 divided by the corresponding number density of nitrogen. An averaged rate constant $k_{3a} = 8.5 \times 10^{-29}$ is derived from the data shown in Table 4.

It should not be overlooked that N_4^+ ions can also dissociate upon collisions. In fact, Varney [22] has successfully interpreted drift velocity data in nitrogen on the basis that N_2^+ and N_4^+ ions are in thermal equilibrium. It remained, therefore, to check upon this possibility under the present experimental conditions. With the use of the equilibrium constant and the temperature scale for N_4^+ ions given by Varney, the degree of dissociation of N_4^+ ions was found inappreciable. Further, an attempt to fit the present data into a thermal equilibrium scheme failed both qualitatively and quantitatively. The conclusion is that the ion residence time in the source is insufficient for equilibrium conditions to develop. On the other hand, this is precisely the situation which enables the determination of the rate constant associated with Reaction (3a).

As with the case of reaction (2) in the present experiments, no evidence for the occurance of reaction (4) could be obtained even under favorable experimental conditions. These experiments were performed with radiation in the 835 to 1000Å region where oxygen is ionized but nitrogen is not. With air being introduced into the ion source of pressures up to 250 microns and with the mass spectrometer trained to register m/e = 30, weak currents were observed, but those did not correlate with the simultaneously recorded optical spectrum in the indicated wavelength region. It is believed that these currents are caused

by the interference of the second order spectrum. Indeed, small N_2^+ currents were also recorded dispite the fact that the limit of ionization for nitrogen is 795Å. The second order radiation falling into the first order 800 to 1000Å region is equivalent to 400 to 500 Å and is capable of producing O^+ by ionization of oxygen, so that NO^+ can in principle be formed from the reaction of atomic oxygen ions with nitrogen. From the current ratio of the background at m/e = 30 to that of the O_2^+ peak and the measured residence time of (O_2^+) in air the upper limit rate constant for reaction (4) is found to be $k_4 \leq 3 \times 10^{-15}$ cc/mol sec.

Reaction (5) was studied mainly to provide an additional check on the applicability of the present techniques. With hydrogen admitted to the source, the N_2^+ and H_3^+ ion intensities observed varied with pressure as shown in Figure 14. The repeller potential in this case was one volt, resulting in a field of approximately 1.5 volt/cm. The pressure dependence resembles that found by Saporoschenko, [27] who used an ion pathlength of 0.5 cm and 4 volt repeller potential. The H_2^+ - H_3^+ conversion is essentially complete at 50 microns pressure. The mode of ionic motion in this pressure domain is predominantly collision-free acceleration. Indeed, residence times derived from first arrival measurements of the ion pulse were found to be pressure independent. Accordingly, Equation (4) has to be applied to correct for the pulse broadening due to the initial thermal velocities of the produced ions. As has been pointed out, the residence time for hydrogen ions is of the same magnitude as the duration of the light pulse; however, first arrival time measurements should still give essentially correct residence times. The average residence time thus deduced is 1.1 μsec, in close agreement with the value calculated from the assumed electric field. The average rate constant derived from the data shown in Figure 14 is $k_5 = 1.85 \times 10^{-9}$ cc/mol sec, in good agreement with the experimental value of 2×10^{-9} cc/mol sec goven by Reuben and Friedman [28] for low repeller fields, and with the value calculated from theory [29] and [30]. The agreement with Saporoschenko's data is less satisfactory, but his measurements were made at higher fields and correspondingly smaller residence times. His results are more in accord with Giese and Maier's [31] data, which approach the theoretical value as the ion velocities are lowered toward the thermal range.

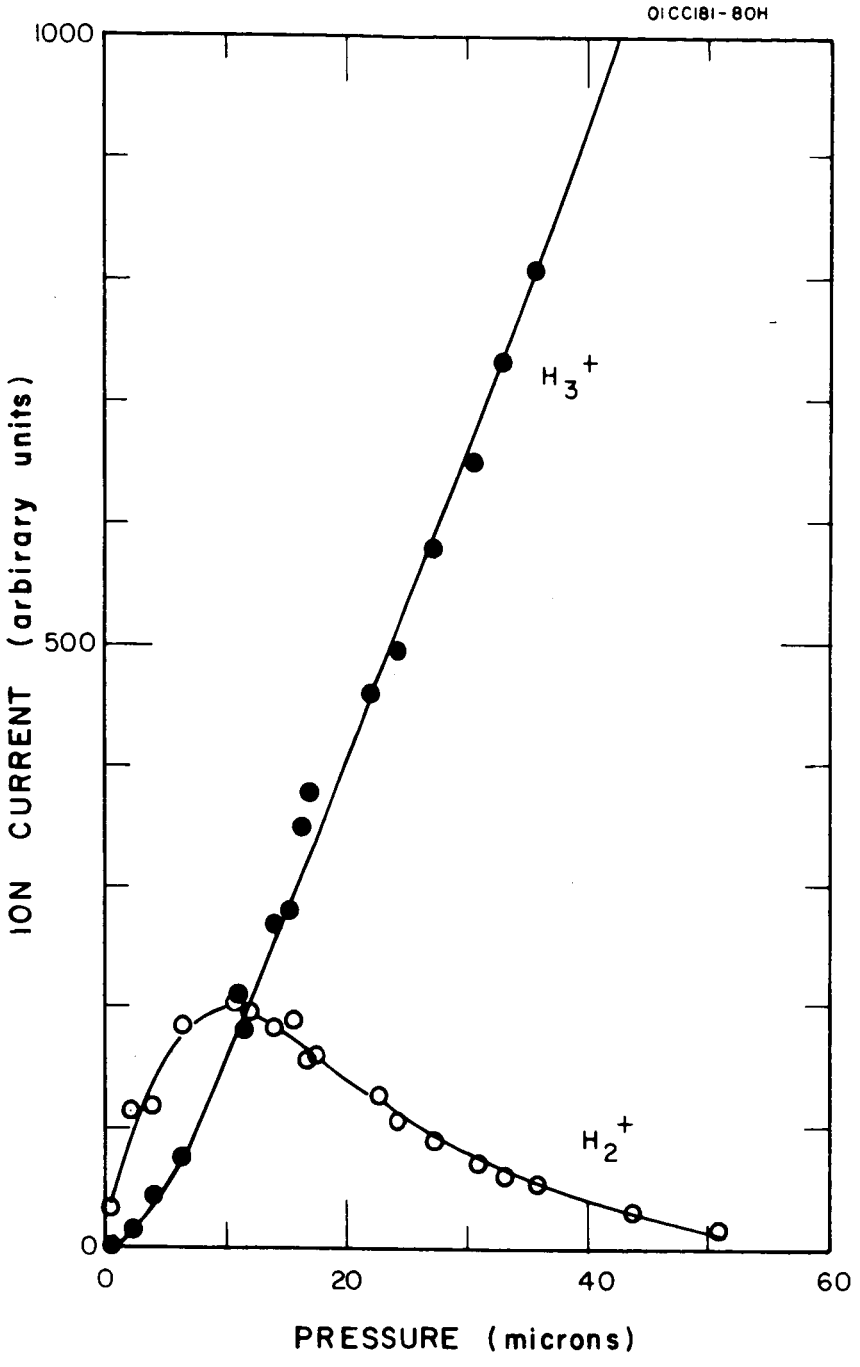

Figure 14. Variation of ion intensities in hydrogen; as a function of pressure.

A VARIETY OF CHARGE TRANSFER PROCESSES

Experimental Procedure

The reactions discussed in this section were obtained by an experimental technique somewhat different from that described in the preceeding section. Accordingly, a description of the additional experimental details pertinent to this investigation is in order.

A fixed flow of the gas from which parent ions were generated by photoionization was introduced to the ion source at 15-20 microns pressure. The neutral reactant was admixed in varying amounts through a second inlet. The gas mixture was ionized by dispersed uv radiation using intermittent light generated in a spark discharge in nitrogen. The wavelength was adjusted to fall in the vicinity of the ionization onset for the parent ion. A repeller potential of one volt corresponding to a field strength approximately 1.6 volt/cm was applied to extract the ions from the source.

The desired rate constants were calculated from the loss of parent ion intensity observed upon admixture of the neutral gaseous reactant. Product ion intensities were determined in conjunction with parent ion loss measurements. However, since product ions were also generated by direct photoionization of the admixed gas, it was necessary to determine this effect separately. The extent of product ion formation due to the reaction was assessed from the difference of the ion currents measured when argon was present and when it was absent.

Partial pressures of the neutral reactant were determined by subtraction of the known pressure of argon from the total pressure. The usable pressure range was dictated primarily by the accuracy of the employed McLeod gauge. Total pressures ranging from 15 to 60 microns were found most suitable. In this pressure region, the motion of the ions is still governed by acceleration in the repeller field and impeding collisions are almost negligible. Parent ion residence times were, therefore, determined from first arrival times of an ionic pulse at the mass spectrometer collector in the manner described previously. Correction was applied for the effect of initial thermal velocities of the ions. Residence times thus obtained varied little over the employed pressure region, except in its uppermost portion, where the influence of collisions became noticeable. The influence of collisions mainly reduced the width of the local ion concentration profile caused by the initial thermal velocity component, but this effect then invalidated the applied correction procedure. Accordingly, residence times were determined at several pressures within the domain where the influence of collisions was still inappreciable, and the averaged residence time was taken to apply to the entire investigated pressure region. No inconsistencies were encountered by the use of this procedure.

Results

Rate constants are given for the charge transfer reactions

(6) $He^+ + N_2 \rightarrow N_2^+ + He$

(7) $He^+ + N_2 \rightarrow N^+ + N + He$

(8) $He^+ + O_2 \rightarrow O_2^+ + He$

(9) $He^+ + O_2 \rightarrow O^+ + O + He$

(10) $A^+ + O_2 \rightarrow O_2^+ + A$

(11) $A^+ + CO_2 \rightarrow CO_2^+ + A$

(12) $N_2^+ + CO_2 \rightarrow CO_2^+ + N_2$

(13) $N_2^+ + NO \rightarrow NO^+ + N_2$

(14) $O_2^+ + NO \rightarrow NO^+ + O_2$

The results are shown in Tables 5 through 11. The above determined rate constants are in very good agreement with the values obtained by other investigators wherever such values are available. For example, the combined rate constants for reactions (6) and (7), and for (8) and (9), are in reasonable agreement with the values $k_6 + k_7 = 1.7 \times 10^{-9}$ and $k_8 + k_9 = 1.5 \times 10^{-9}$ cc/mole sec given by Ferguson and collaborators [32].

However, in the present work, the partitioning between the individual steps could be determined also. As Table 5 shows the reaction of helium ions with nitrogen produces, on the average, 52 percent N^+ and 48 percent N_2^+. Hence, $k_6 = 7.1 \times 10^{-10}$ cc/molecule sec and $k_7 = 7.6 \times 10^{-10}$ cc/ molecule sec. Ferguson, et al., could not measure the exact degree of partitioning because of the prescence of metastable helium atoms in their experiments, and they have assumed that reaction (7) is predominant.

Similarly, it is estimated from the lack of significant amounts of O_2^+ production in the reaction of helium ions with oxygen, that reactions (8) consumes less than 10 percent of the helium ions reacting with O_2. Accordingly, reaction (9) is preponderant. The ratio $(k_6 + k_7)/(k_8 + k_9) = 1.25$ is in excellent agreement with that found by Ferguson et al., [32] $(k_6 + k_7)/(k_8 + k_9) = 1.2$.

It is significant that the reaction of helium ions with nitrogen results in a very good product balance, whereas the reaction with oxygen is not. The

TABLE 5

REACTION OF HELIUM IONS WITH NITROGEN

IONIZING WAVELENGTH 482Å

$P(N_2)$ (microns)	He^+	ΔHe^+	ΔN^+	ΔN_2^+	$\Delta N^+ + \Delta N_2^+$	t	$k \times 10^9$
	(Arbitrary Units)					μsec	cc/molecule sec
0	330	0	0	0	0	2.3	-
2.0	285	45	28.5	22	50.5	"	1.02
3.5	232	98	54.5	51	105.5	"	1.36
5.0	188	142	76	70.5	146.5	"	1.49
7.5	140	190	102	95	197	"	1.51
9	115	215	114	108	222	"	1.55
10	96	234	117	120	237	"	1.62
13	73.5	256.5	136	127	263	"	1.52
15	56	274	148	134	282	"	1.56
17.5	43	287	153	143	296	"	1.52
19	34.5	295.5	153	150	303	"	1.56

$(\Delta N^+ + \Delta N_2^+)/\Delta He^+ = 1.04$ Average $k_6 + k_7 = 1.47 \times 10^{-9}$

TABLE 6

REACTION OF HELIUM IONS WITH OXYGEN

IONIZING WAVELENGTH 482Å

$P(O_2)$ (microns)	He^+	$\Delta(He^+)$ (Arbitrary Units)	$\Delta(O^+)$	t μsec	$\log \frac{He_o^+}{He^+}$	$k_3 \times 10^9$ cc/molecule sec
0	330	0	0	2.3	-	-
4	220	110	16	"	0.178	1.34
6	192	138	19	"	0.238	1.20
8	178	152	23	"	0.270	1.02
9	139	191	26	"	0.377	1.27
11	124	206	28.5	"	0.427	1.17
13	111	219	28	"	0.474	1.10
15	87.5	242.5	33	"	0.578	1.17
18	66	264	35	"	0.701	1.18
21	51	279	38	"	0.812	1.17
22	42	288	37.5	"	0.898	1.24

$\Delta O^+/\Delta He^+ = 0.14$ Average $k_9 = 1.18 \times 10^{-9}$

TABLE 7

REACTION OF ARGON IONS WITH OXYGEN

IONIZING WAVELENGTH 780Å

Pressure microns	$P(O_2)$	A^+ (Arbitrary Units)	ΔA^+	ΔO_2^+	τ μsec	$\lg \frac{A_o^+}{A^+}$	$k \times 10^{-10}$ cc/molecule sec
16.5	0	165	0	0	9.0	-	-
19.5	3.0	149	16	15	"	0.044	1.13
23	6.5	135	30	27	"	0.087	1.04
25.5	9.0	123	42	38	"	0.128	1.10
29.5	13	111	54	54	"	0.172	1.02
31	14.5	96	69	56	"	0.235	1.25
34.5	18	91	74	70	"	0.258	1.11
38.5	22	79.5	85.4	76	"	0.318	1.12
43	26.5	69	96	87	"	0.379	1.11
48.5	32	58	107	97	"	0.454	1.09
55	38.5	48	117	114	"	0.536	1.08

Average $\Delta O_2^+ / \Delta A^+ = 0.92$

Average $k_{10} = 1.10 \times 10^{-10}$

TABLE 8

REACTION OF ARGON IONS WITH CO_2

IONIZING WAVELENGTH 780Å

Pressure microns	$P(CO_2)$	A^+ (Arbitrary Units)	ΔA^+	ΔCO_2^+	τ μsec	$\lg \frac{A_o^+}{A^+}$	$k \times 10^{-10}$ cc/molecule sec
13	0	234	0	0	7.9	-	-
14	1	189	45	20	"	0.092	8.10
15	2	164	70	32	"	0.155	6.82
16.5	3.5	126	108	50	"	0.269	6.78
18	5	102	132	70	"	0.361	6.40
19.5	6.5	75	159	76	"	0.494	6.74
20	7	60	174	85	"	0.592	7.46
21.5	8.5	51.5	182.5	87	"	0.658	6.84
23	10	40	194	90	"	0.767	6.77
25.5	12.5	26	208	98	"	0.954	6.74
27	14	19	215	104	"	1.091	6.88
28	15	16.5	217.5	104	"	1.194	7.03

Average $\Delta CO_2^+/\Delta A^+ = 0.48$

Average $k_{11} = 7.0 \times 10^{-10}$

TABLE 9

REACTION OF NITROGEN IONS WITH CO_2

IONIZING WAVELENGTH 480Å

Pressure $P(CO_2)$ microns		N_2^+ (Arbitrary Units)	$\triangle N_2^+$	$\triangle CO_2^+$	τ μsec	$\lg \frac{(N_2^+)_o}{(N_2^+)}$	$k \times 10^{-10}$ cc/molec sec
20	0	162	0	0	8.7	-	-
20.5	0.5	140	22	19	"	0.062	9.95
21.5	1.5	108	54	46	"	0.177	9.45
22.5	2.5	85	77	58	"	0.281	9.00
23.5	3.5	70	92	66	"	0.365	9.08
24.5	4.5	51	111	83	"	0.501	8.93
25.5	5.5	40.5	121.5	91	"	0.602	8.78
27.0	7.0	27.5	134.5	86	"	0.769	8.80
28	8.0	21	141	107	"	0.887	8.88

Average $\triangle CO_2^+ / \triangle N_2^+ = 0.76$

Average $k_{12} = 9.1 \times 10^{-10}$

TABLE 10

REACTION OF NITROGEN IONS WITH NO

IONIZING WAVELENGTH 780Å

P (NO) (microns)	N_2^+ (Arbitrary Units)	ΔN_2^+ (Arbitrary Units)	ΔNO^+ (Arbitrary Units)	τ μsec	$\lg \frac{(N_2^+)_o}{(N_2^+)}$	$k_1 \times 10^{-10}$ cc/mole sec
0	146	0	0	-	-	-
1	129	17	15	7.4	0.056	5.28
2.3	111	35	24	-	0.122	5.0
3	102	44	32	-	0.158	4.95
4	91	55	40	-	0.207	4.88
4.5	96	50	45	-	0.184	3.85
6	72	74	60	-	0.309	4.85
7.5	62	84	58	-	0.374	4.7
9	53.5	92.5	65	-	0.438	4.6
11.5	38	108	76	-	0.587	4.85
15	24	122	94	-	0.786	4.95

$\Delta NO^+ / \Delta N_2^+ = 0.76$

Averafe $k_{13} = 4.8 \times 10^{-10}$

TABLE 11

REACTION OF OXYGEN IONS WITH NO

IONIZING WAVELENGTH 980Å

P (NO) (microns)	O_2^+ (Arbitrary Units)	ΔO_2^+ (Arbitrary Units)	ΔNO^+ (Arbitrary Units)	sec	$\lg \frac{(O_2^+)_o}{(O_2^+)}$	k_2 cc/molecule sec
0	145	0	0	-	-	-
0.5	129	16	12	6.4	0.053	11.50
1.5	108	37	40	-	0.130	9.50
3.0	90	55	50	-	0.210	7.62
3.5	96	49	45	-	0.182	5.65
4.5	75	70	65	-	0.288	7.02
6.5	53.5	91.5	80	-	0.436	7.34
8.0	45	100	100	-	0.510	7.02
9.5	35	110	95	-	0.618	7.12
11.0	27.5	117.5	100	-	0.724	7.23
12.0	24	121	100	-	0.784	7.23

$\Delta NO^+/\Delta O_2^+ = 0.90$ Average $k_{14} = 7.7 \times 10^{-10}$

sum of the product ion intensities N_2^+ and N^+ match the helium ion losses within 5 percent error. This indicates that mass discrimination at the electron multiplier is negligible. This result is in agreement with our previous results obtained by a different method. On the other hand, from the values shown in Table 6 it can be demonstrated that a mass balance for the reaction with oxygen is not operative. On the average, the ratio of O^+ ions detected compared with helium ions consumed is only 0.14 or about one seventh of that expected. It is clear that, in principle, the discrepancies could be due to the formation of additional products other than those identified, but a search for other products was unsuccessful. Specifically, such ionic species as HeO^+ and HeO_2^+ could not be detected. Also, the amount of impurity ions present was grossly insufficient to account for the observed discrepancies.

From our previous discussion it appears that the decrease in the ion collection efficiency for ions with excess kinetic energy could be held responsible for the observed discrepancy. Accordingly, a series of retarding potential measurements were made on ions leaving the ion source. For this purpose, a grid was inserted between the ion source and the first ion accelerating electrode. It was found that He^+ and O_2^+ ions acquire the energy imparted to them by the 0.5 eV drift field applied inside the ion source but not more. On the other hand, the O^+ ion current produced either by photoionization at 482Å or by reaction (9) contains an appreciable fraction of atomic oxygen ions with excess kinetic energy. Product imbalance observed for reaction (9) is, therefore, attributed to energy discrimination in the ion source.

The present results for reactions (10), (13), and (14) are also in good accord with the previous data obtained by Ferguson and collaborators [33,34]. No previous values appear to be available for reactions (11) and (12). Interestingly, the results for reactions (11) through (13) also indicate product imbalance. In view of the experience gained with the reactions of helium ions the observation is again interpreted as being due to ions carrying excess kinetic energy, although in these cases no specific attempts were made to verify the existence of fast product ions.

Discussion

Although the present data show little scatter, and even though good agreement is obtained in the cases where comparison with previous values is possible, it is believed that the derived rate constants are only moderately accurate because of the various corrections applied in determining parent ion residence times. An estimate places the combined systematic error at 25 percent.

The maximum energy acquired by an ion moving in the repeller field is given by the pertinent accelerating potential. From the applied repeller potential, the repeller position, and the flight distance from the parent ion origin to the extraction orifice, the maximum energy for ions leaving the source is, for the present experiments, estimated as $U_d = 0.5$ eV. This, however, is not the energy which, on the average, ions have acquired when they

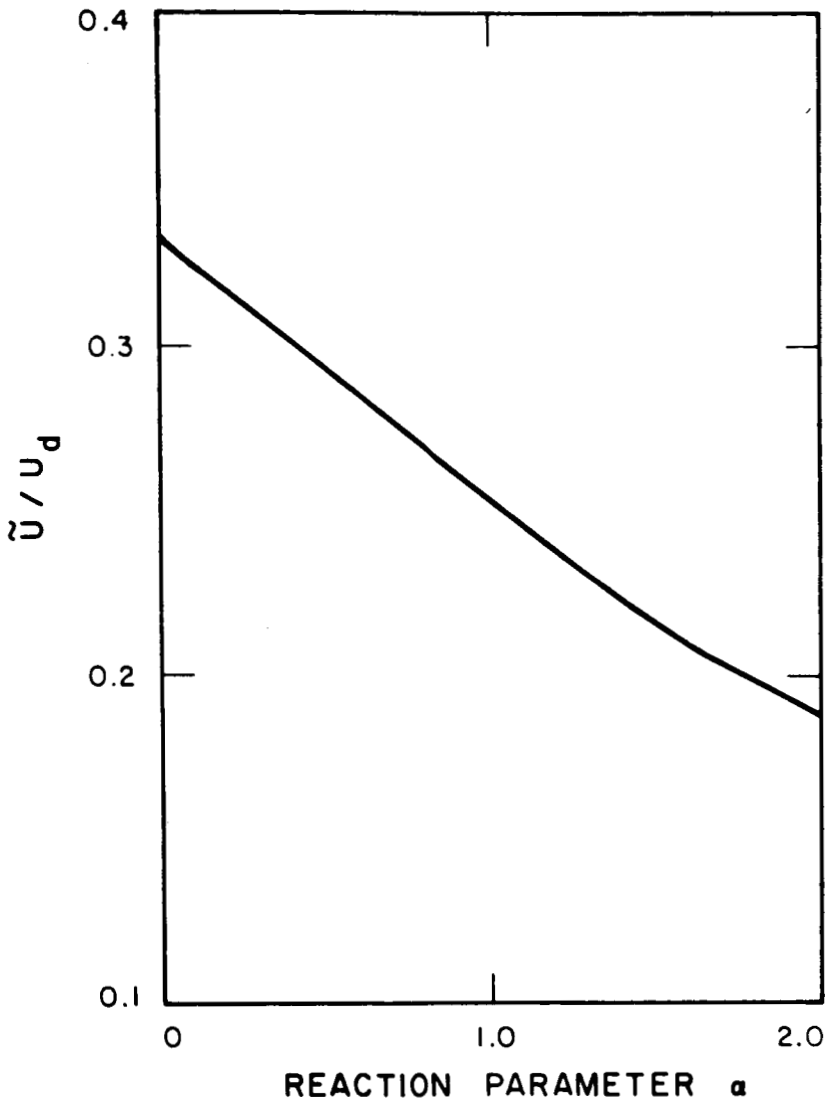

Figure 15. Normalized average energy of reacting ions $U/U_d = I(\alpha)$ as a function of the reaction parameter $\alpha = kA\tau$.

undergo a reaction, because the reaction probability decreases as the ions approach the extraction orifice due to their increasing velocity on one hand and their decreasing concentration on the other. The average energy of the reacting ions is derived in Appendix B. It is assumed that the average initial (thermal) energy of the ions can be neglected. The average energy of reacting ions is found to be proportional to the applied accelerating potential and to a function F of the parameter $\alpha = kA\tau$, where k is the rate constant associated with the reaction, A the neutral reactant number density, and τ the parent ion residence time. The function $F(\alpha)$ is plotted in Figure 15. For $\alpha \approx 0$, when the degree of reaction is so small that the decrease in parent ion intensity is still inappreciable, the average energy of ions undergoing reaction is $\tilde{U} = 0.33\ U_d$. With increasing α, the average energy decreases. The maximum value of α reached in the present experiments is around $\alpha = 1.3$, where $\tilde{U} = 0.23\ U_d$. Accordingly, the range of average energies of the reacting ions is 0.115 to 0.166 eV. These values must be considered approximate, since at such low energies, it is no longer admissible to neglect the average initial energy of the ions. The present range of energies lies appreciably above that found previously for N_2^+ ions in air at higher pressures, although it is still in the thermal energy range. Owing to the non-Maxwellian energy distribution of reacting ions, no attempt is made to represent the average energies by equivalent temperatures.

Despite the fact that the change in average energy with increasing α amounts to only 35 percent, it is significant that the rate constants are independent of the average energy. Since the rate constant k for a reaction is related to the reaction cross section $\sigma(v)$ by

$$k = \int_0^\infty v\ \sigma(v)\ f(v)\ dv$$

where v is the relative velocity of the interacting particles, and f(v) is the appropriate normalized distribution function, the invariance of k with energy indicates that the product $v\ \sigma(v)$ is essentially constant for sufficiently slow ions. The validity of the $\sigma \propto 1/v$ law for low energy collisions has been discussed in a theoretical context by Rapp and Francis [35] and by Takayanagi [36]. Since this is also an implication in the theory of thermal ion-molecule reactions, put forth by Gioumousis and Stevenson [37], it is of interest to compare the present experimental rate constants with the corresponding theoretical values. From the theory, k is given by

$$k = 2\pi\ e(\alpha/\mu)^{1/2}$$

where e is the charge of the ion, α the polarizability of the neutral reactant, and μ the reduced mass of the reaction participants. Also implicit in this equation is the assumption that all sufficiently close encounters lead to reaction. If this is not the case, the introduction of a probability factor R is required which corresponds to the transmission coefficient in the older theory by Eyring, Hirschfelder, and Taylor [38].

The data for the investigated reactions are summarized in Table 12. The polarizabilities used in the computations were taken from the tabulations by Maryott and Buckley [39]. It is apparent that the observed rate constants are all smaller than the theoretical ones, although the order of magnitude is generally preserved. However, since the computed rate constants are in reality only upper limit values, it appears that the experimental rate constants are in reasonable agreement with theory and that the differences should be attributed to varying reaction probability factors. Ratios of experimental to theoretical rate constants, which would signify the individual probability factors, are also entered in Table 12. According to these ratios, the reaction of nitrogen ions with carbon dioxide and that of oxygen ions with NO are the most efficient, whereas the reaction of nitrogen ions with oxygen is the least efficient.

Several years ago, Massey [40] put forth the hypothesis that the character of low energy collisions is adiabatic. and by use of a correspondence principle argument, he suggested that cross sections for charge transfer under gas kinetic conditions would be extremely small unless the energy change ΔE in the involved electronic transitions is small; large cross sections should be expected only in the cases of resonance. The present results argue strongly against this point. Column 3 of Table 12 shows reaction cross sections calculated from $\sigma = k/v$ for the maximum average energy of reacting ions $\tilde{U} = 0.166$ eV. The resulting cross sections are comparable to gas kinetic values. Also, the one reaction having the smallest energy defect, the reaction of argon ions with nitrogen, has the smallest cross section, contrary to expectation according to the adiabatic hypothesis. Paulson [41] has previously pointed out that the Massey hypothesis appears to fail at low energies for those processes in which ion induced dipole forces dominate, because then an intermediate complex of lifetime greater than one vibrational period can be formed. This is also the position taken by Light [42,43] who used a phase space formulation to evaluate the probability of the various decay modes of the intermediate complex, and who has derived energy dependencies of cross sections in surprisingly good agreement with experimental data in many cases. On the other hand, it should be realized that Massey's hypothesis was originally formulated for atomic collisions where, except for symmetrical systems, resonances are coincidental and few, and where this hypothesis had its greatest measure of success. Molecules, by comparison, possess many close-lying, electronic, vibrational and rotational levels, so that the probability of near resonance is considerably increased. The present observation that reaction systems with a large energy defect ΔE, such as the charge transfer process involving argon ions and nitric oxide have large cross sections, may reflect the possibility of excited secondary ion formation. A judgement concerning this point must be reserved until more experimental details are available on the nature of the product ions evolved from such reactions. The indication in the present work that exothermic reactions may result in product ions having appreciable excess kinetic energy, also suggests the importance of energetic considerations and calls for more detailed investigations of this effect.

TABLE 12

COMPARISON OF RESULTS WITH THEORY

Reaction	ΔE (eV)	$\sigma^* \times 10^{16}$ (cm^2/molecule)	$k_{exp} \times 10^{10}$ (cc/molecule sec)	$k_{theor} \times 10^{10}$	k_{exp}/k_{theor}
$He^+ + N_2$	9.0	530	15	16.5	0.91
$He^+ + O_2$	12.37	420	12	15.5	0.77
$A^+ + O_2$	3.54	12	1.1	6.92	0.16
$A^+ + CO_2$	1.96	78	7.0	8.75	0.80
$N_2^+ + O_2$	3.37	15	1.1	7.55	0.15
$N_2^+ + CO_2$	1.79	121	9.1	9.67	0.94
$N_2^+ + NO$	6.33	64	4.8	8.45	0.57
$O_2^+ + NO$	2.96	96	7.7	8.17	0.94

σ^* for ions of 0.166 eV energy

CONCLUSIONS

The present investigation differs from previous mass spectrometer investigations of ion-molecule reactions in two respects: (a) photoionization replaces the more commonly employed electron impact mode of ion formation and (b) a new technique is employed for the determination of ion residence times in the source in the presence of a constant repeller field. The ensuing advantages are: the state of the primary ions is reasonably well defined by the choice of ionizing wavelength and residence times can be obtained without a detailed knowledge of the electric field configuration in the ion source. This is particularly valuable at higher pressures where residence times are not calculable form Newton's formula. The interpretation of ion pulse shapes in terms of ion density distributions enables the determination of ion diffusion coefficients from the broadening of the density profile, and ultimately the derivation of approximate ion temperatures. It is an important finding that at pressures above 50 microns, where the basic motion of ions is drift in the electric field, the ionic temperatures are in the thermal range provided only moderate fields are applied. Finally, rate constants for several reactions involving helium argon nitrogen, oxygen and hydrogen ions are given and compared with existing data where available. Satisfactory agreement is obtained in all cases, indicating that the methods applied here are useful in extending rate constant determinations toward higher pressures than was previously thought possible.

APPENDIX A

CORRECTION FORMULA FOR THE DETERMINATION OF RESIDENCE TIMES

To evaluate the effect of diffusion on a group of ions moving in the source under the influence of a field, consider the following idealized physical situation. It is assumed that ions are deposited by a delta source release at the instant $t = 0$ in the plane $x = 0$, and that a one-dimensional Gaussian ion concentration profile develops due to diffusive motion perpendicular to the plane of origin:

$$n(x,t) = N_o(4\pi Dt)^{-1/2} \exp(-x^2/4Dt)$$

Here, x is the distance from the center of the profile, N_o is the total number of ions generated per unit area in the plane of origin, and D is the diffusion coefficient.

Superimposed upon diffusion is the motion of ions toward the sampling orifice due to the applied electric field. Since the field is also perpendicular to the plane of origin, it is convenient to express x in terms of the drift velocity v and the time t. In the pressure region where diffusion occurs, the drift velocity is constant, so that $x = d - vt$ with d being the known distance from the center of the light beam to the sampling aperture. If the average residence time $\tau_o = d/v$ is introduced, $x = d(1 - t/\tau_o)$.

Consider now the flux of ions entering the sampling aperture. The contributions of both drift and diffusion give the flux

$$Q(v,t) = vn(x,t) - D\frac{\partial n(x,t)}{\partial t} = vn(x,t) + \frac{xn(x,t)}{2t}$$

The buildup of charge at the detector located behind the sampling aperture is given by the time integral

$$P(v,t) = \int_o^t Q(v,t)\,dt = \int_o^t n(x,t)\,(v + x/2t)\,dt$$

which can be evaluated to yield

$$P(v,t) = 1/2\,N_o\,[1 - \mathrm{erf}\,(x/2\sqrt{Dt})]$$

The determination of the time $t = \tau$ at which ions are first detected requires the definition of a threshold. Since experience has shown that the average practical detection limit is around ten percent of the total pulse height

displayed on the oscilloscope, it is reasonable to set $P(v,t) = 0.1\ N_o$ and evaluate the error function accordingly. This leads to

$$0.906 = x/2\sqrt{D\tau} = d(1-\tau/\tau_o)/2\sqrt{D\tau}$$

which can be rearranged to yield

$$\tau_o = \tau/[1 - (1.28/d)\sqrt{2D\tau}\ ]$$

In the low pressure region where the motion of ions is governed by collision-free acceleration in the electric field, the broadening of the ion concentration profile is due to the thermal distribution of initial ion velocities, and

$$n(x,t) = \frac{N_o}{t}\left(\frac{m}{2\pi kT}\right)^{1/2} \exp\left(-\frac{m}{2kT}\frac{x^2}{t^2}\right)$$

Here, m is the mass of the ion, k the Boltzmann constant, and T the temperature. The flight velocity is no longer constant, but the acceleration, a, provided by the field is. Similarly as above, $x = d - at^2/2 = d(1-t^2/\tau_o^2)$ and by the same arguments, one derives for this case

$$\tau_o^2 = \tau^2/[1 - (1.28\tau/d)\sqrt{kT/m}\ ]$$

APPENDIX B

AVERAGE ENERGY OF REACTING IONS

To determine the average energy that ions have gained in the field at the moment of reaction, consider first the probability of reaction as a function of time after the deposition of ions in the plane x = 0. If the process under consideration is written

$$N^+ + A \rightarrow M^+ + B$$

the probability of reaction at any instant t is

$$\delta M^+ = kN^+ A\delta t$$

where k is the associated rate constant and M^+, N^+, and A stand for the concentrations of the respective species. Since further $\delta M^+ = -\delta N^+$, the integrated rate equation yields

$$\delta M^+ = kAN_o\, e^{-kAt}\, \delta t$$

and

$$M^+ = N_o(1 - e^{-kAt})$$

with $N_o = M^+ + N^+$ being the initial concentration of parent ions in the plane x = 0 at the instant t = 0. Thus, one can define the normalized reaction probability

$$\delta\Phi = \Phi(t)\, \delta t = \frac{kA\, e^{-kAt}}{1 - e^{kA\tau}}\, \delta t$$

with $\Phi(\tau) = 1$, where τ is the total residence time of parent ions N^+ in the source. It is convenient to introduce the parameter $\alpha = kA\tau$ as a measure of the reaction rate. Then,

$$\Phi(t)\, \delta t = \frac{\alpha}{\tau} \frac{e^{-\alpha t/\tau}}{1 - e^{-\alpha}}$$

If the influence of collisions upon the motion of ions can be neglected and if the initial kinetic energy of ions being accelerated in the electric field is negligible in comparison to the energy acquired at the moment of reaction, the energy of a parent ion at the instant t is given by

$$U = e^2 E^2 t^2/2m = e\, Edt^2/\tau^2$$

where e is the charge of the electron, E the electric field strength, m the mass of the ion, and d the distance from the origin of the ions to the extraction orifice in the source. The total acceleration potential experienced by the ions is e Ed = U_d. The average energy of the ions reacting at any time t with $0 < t < \tau$ is

$$\tilde{U} = \int_0^\tau U(t)\ \Phi(t)\ \delta t$$

$$= \frac{\alpha\ U_d}{\tau^3(1 - e^{-\alpha})} \int_0^\tau t^2\ e^{-\alpha t/\tau}\ \delta t$$

Evaluation of the integral leads to the expression

$$\tilde{U} = U_d\ F(\alpha) = U_d\ \frac{2 - (\alpha^2+2\alpha+2)\ e^{-\alpha}}{\alpha^2(1 - e^{-\alpha})}$$

which relates $\tilde{U}$ to α. The function $F(\alpha)$ is plotted in Figure 15.

REFERENCES

1. Hasted, J.B., in Advances in Electronics and Electron Physics XIII, 1, ed. L. Marton, Academic Press, New York (1960).

2. Lampe, F.W., J.L. Franklin, and F.H. Field, in Progress in Reaction Kinetics 1, 69, ed. G. Porter, Pergamon Press, Oxford (1961).

3. Melton, C.E., in Mass Spectrometry of Organic Ions, ed. F.W. McLafferty, Academic Press, New York (1963).

4. Stevenson, D.P. in Mass Spectrometry, ed. C.A. McDowell, McGraw Hill, New York (1963).

5. Paulson, J.F., Ann. de Geophysique 20, 75 (1964).

6. Talrose, V.L. and E.L. Frankevich, Zh. Fiz. Khim. 34, 2709 (1960). This pulse method has also been used by others to study ion formation in reactions of excited atoms.(14-16)

7. Hand,C.W. and H. von Weyssenhoff, Can. J. Chem. 42, 195 (1964); 42, 2385 (1964).

8. Weissler, G.L., J.A.R. Samson, M. Ogawa, and G.R. Cook, J. Opt. Soc. Am. 49, 338 (1959).

9. Hurzeler, H., M.G. Inghram, and J.P. Morrison, J. Chem. Phys. 27, 313 (1958); 28, 76 (1958).

10. Schoen, R.I., J. Chem. Phys. 37, 2032 (1962).

11. Comes, F.J. and W. Lessmann, Z. Naturforschung 19a, 65 (1964).

12. Dibeler, V.H. and R.M. Reese, J. Res. Natl. Bur. Std. 68a, 409 (1964).

13. Poschenrieder, W and P. Warneck, "Gas Analysis by Photoionization Mass Spectrometry" GCA Tech. Rep 66-1-N, Contract No. NASW-1283 (1966).

14. Samson, J.A.R. and R.B. Cairns, J. Geophys. Res. 69, 4583 (1964); 70, 99 (1965).

15. Cook, G.R. and P.H. Metzger, J. Opt. Soc. Am. 54, 968 (1964).

16. Metzger, P.H. and G. R. Cook, J. Chem. Phys. 41, 642 (1964).

17. Dibeler, V.H., M. Krauss, R.M. Reese, and F.N. Harllee, J. Chem. Phys. 42, 3791 (1965).

18. Ferguson, E.E., F.C. Fehsenfeld, D.B. Dunkin, A.L. Schmeltekopf, and H.I. Schiff, Planet. Space Sci. 12, 1169 (1964).

19. Moran, T.F. and L. Friedman, J. Geophys. Res. 70, 4992 (1965).

20. Martin, D.W., W.S. Barnes, G.E. Keller, D.S. Harmer, and E.W. McDaniel, Proc. VI Intern. Conf. Ionization Phenomena in Gases, p. 295, Paris (1963).

E.W. Daniel, G.E. Keller, D.L. Albritton, T.M. Miller and D.W. Martin have presented more refined results at the "IV the International Conference on the Physics of Electronic and Atomic Collisions" Quebec, Canada (1965). These more recent results an slightly lower than those shown in Figure 9.

21. Dahlquist, J.A., J. Chem. Phys. 39, 1203 (1963).

22. Varney, R.N., J. Chem. Phys. 31, 1314 (1959).

23. Fite, W.L., J.A. Rutherford, W.R. Snow, and V.A. J. van Lint, Discussion Faraday Soc. 33, 264 (1962).

24. Fehsenfeld, F.C., A.L. Schmeltekopf, and E.E. Ferguson, Planet. Space Sci. 13, 919 (1965).

25. Galli, A., A. Giardini-Guidoni, and G.G. Volpi, J. Chem. Phys. 39, 518 (1963).

26. Talrose, V.L., M.I. Markin, and I.K. Larin, Disc. Faraday Soc. 33, 257 (1962).

27. Saporoschenko, M., J. Chem. Phys. 42, 2760 (1965).

28. Reuben, B.G. and L. Friedman, J. Chem. Phys. 37, 1636 (1962).

29. Eyring, H., J.O. Hirschfelder, and H.S. Taylor, J. Chem. Phys. 4, 479 (1936).

30. Gioumousis, G. and D.P. Stevenson, J. Chem. Phys. 29, 294 (1958).

31. Giese, C.F. and W.B. Maier, J. Chem. Phys. 39, 739 (1963).

32. Ferguson, E.E., F.C. Fehsenfeld, , A.L. Schmeltekopf, and H.I. Schiff, Planet. Space Sci. 12,1169 (1964).

33. Fehsenfeld, F.C., A.L. Schmeltekopf, G.I. Gilman, L.G. Puls and E.E. Ferguson, 18th Gasious Electronics Conference, Minneapolis, Minnesota (1965).

34. Ferguson, E.E., F.C. Fehsenfeld, P.D. Goldan and A.L. Schmeltekopf, J. Geo. Res. Vol. 70, p.4323 (1965).

35. Rapp, D. and W.E. Francis, J. Chem Phys. 37, 2631 (1962).

36. Takayanagi, K. Sci. Rept. Saitama Univ. A4, 41 (1962).

37. Gioumousis G. and D.P. Stevenson, J. Chem. Phys. 29, 294 (1958).

38. Eyring, H. J. O. Hirschfelder, and H.S. Taylor, J. Chem. Phys. 4, 479 (1936).

39. Maryott, A.A. and F. Buckley, "Table of Dielectric Constants and Electric Dipole Moments" NBS Circular 537 (1963).

40. Massey, H.S. W. and E.H. S. Burhop, Electronic and Ionic Impact Phenomena (Clarendon Press, Oxford, 1956) p. 441.

41. Paulson, J.F., Ann. de Geophys. 20, 75 (1964).

42. Light, J.C., J. Chem. Phys. 40, 3221 (1964).

43. Light, J.C., and J. Liu, J. Chem. Phys. 43, 3209 (1965).